



1 **Oceanographic regional climate projections for the Baltic Sea**
2 **until 2100**

3 H. E. Markus Meier^{1,2}, Christian Dieterich^{2,†}, Matthias Gröger¹, Cyril Dutheil¹, Florian
4 Börgel¹, Kseniia Safonova¹, Ole B. Christensen³ and Erik Kjellström²

5 ¹Department of Physical Oceanography and Instrumentation, Leibniz Institute for Baltic Sea Research
6 Warnemünde, Rostock, 18119, Germany

7 ²Research and Development Department, Swedish Meteorological and Hydrological Institute, Norrköping, 601
8 76, Sweden

9 ³Danish Climate Center, Danish Meteorological Institute, Copenhagen, Denmark

10 [†]Deceased

11

12 *Correspondence to:* H.E. Markus Meier (markus.meier@io-warnemuende.de)

13 **Abstract.** Recently performed scenario simulations for the Baltic Sea including marine biogeochemistry were
14 analyzed and compared with earlier published projections. The Baltic Sea, located in northern Europe, is a semi-
15 enclosed, shallow and tide-less sea with seasonal sea ice cover in its northern sub-basins and a long residence
16 time causing oxygen depletion in the bottom water of the southern sub-basins. With the help of dynamical
17 downscaling using a regional coupled atmosphere-ocean climate model, four global Earth System Models were
18 regionalized. As the regional climate model does not include components for the terrestrial and marine
19 biogeochemistry, an additional catchment and coupled physical-biogeochemical model for the Baltic Sea were
20 used. In addition to previous scenario simulations, the impact of various water level scenarios was examined as
21 well. The projections suggest higher water temperatures, a shallower mixed layer with sharper thermocline
22 during summer, reduced sea ice cover and intensified mixing in the northern Baltic Sea during winter compared
23 to present climate. Both frequency and duration of marine heat waves would increase significantly, in particular
24 in the coastal zone of the southern Baltic Sea (except in regions with frequent upwelling). Due to the
25 uncertainties in projections of the regional wind, water cycle and global sea level rise, robust and statistically
26 significant salinity changes cannot be identified. The impact of changing climate on biogeochemical cycling is
27 considerable but in any case smaller than the impact of plausible nutrient input changes. Implementing the
28 proposed Baltic Sea Action Plan, a nutrient input abatement plan for the entire catchment area, would result in a
29 significantly improved ecological status of the Baltic Sea and reduced hypoxic area also in future climate,
30 strengthening the resilience of the Baltic Sea against anticipated future climate change. While our findings about
31 changes in variables of the heat cycle mainly confirm earlier scenario simulations, earlier projections for salinity
32 and biogeochemical cycles differ substantially because of different experimental setups and different
33 bioavailable nutrient input scenarios.

34

35 During the time in which this paper was prepared, shortly before submission, Christian Dieterich passed away
36 (1964-2021). This sad event marked the end of the life of a distinguished oceanographer and climate scientist
37 who made important contributions to the climate modeling of the Baltic Sea, North Sea and North Atlantic
38 regions.

39



40 1 Introduction

41 The Baltic Sea is a shallow, semi-enclosed sea with a mean depth of 54 m located in northern Europe (Fig. 1).
42 Due to the strongly varying bottom topography, the Baltic Sea can be divided into a number of sub-basins with
43 limited transports between sub-basins (Sjöberg, 1992). In particular, the water exchange with the North Sea is
44 hampered because of two shallow sills located in narrow channels connecting the Baltic Sea with the North Sea.
45 Large saltwater inflows occur only sporadically, on average once per year mainly during the winter season but
46 never during summer (Mohrholz, 2018). Furthermore, the Baltic Sea is embedded into a catchment area that is
47 about four times larger than the Baltic Sea surface with a large annual freshwater input relative to the volume of
48 the Baltic Sea (Bergström and Carlsson, 1994) causing large horizontal and vertical salinity gradients (Fonselius
49 and Valderrama, 2003).

50

51 Due to its location and physical characteristics such as the long residence time, the Baltic Sea is vulnerable to
52 external pressures such as eutrophication, pollution, or global warming (e.g., Jutterström et al., 2014). The
53 volume of the Baltic Sea amounts to 21,700 km³ (Sjöberg, 1992) and consequently the turnover time of the total
54 freshwater supply of about 16,000 m³ s⁻¹ (Meier and Kauker, 2003) is about 40 years. Using ocean circulation
55 modeling, the time scale of the salinity response to changes in atmospheric and hydrological forcing was
56 estimated at about 20 years (Meier, 2006).

57

58 In the early 21st century, about 85 million people, in 14 countries, were living in the catchment area,
59 representing a considerable anthropogenic pressure for the marine ecosystem (HELCOM, 2018). Insufficiently
60 treated wastewater, emissions of pollutants, overfishing, habitat degradation, and intensive marine traffic such as
61 oil transports put a heavy burden on the ecosystem of the Baltic Sea (Reckermann et al., 2021). One example is
62 the oxygen depletion of the Baltic Sea deep water, with the consequence of dead sea bottoms lacking higher
63 forms of life (e.g., Carstensen et al., 2014; Meier et al., 2018b). In 2018, the area of the dead bottoms was equal
64 to the size of the Republic of Ireland, with an area of about 73,000 km², which is about one sixth of the sea
65 surface of the Baltic Sea. Bottom oxygen of the deeper parts of the Baltic is depleted because of the limited
66 ventilation of the deep water and because of the accelerated oxygen consumption due to the remineralization of
67 organic matter (Meier et al., 2018b). Hence, nutrient input abatement strategies, the so-called Baltic Sea Action
68 Plan (BSAP) were discussed (HELCOM, 2007) and projections are requested by stakeholders such as the
69 Helsinki Commission (HELCOM) or national environmental protection agencies¹.

70

71 Projections for the Baltic Sea climate at the end of the 21st century were among the first to be made for coastal
72 seas worldwide (Meier and Saraiva, 2020)). Already at the beginning of the 2000s the first scenario simulations
73 based upon dynamical downscaling (Fig. 2) were carried out for selected time slices in present and future
74 climates (e.g., Haapala et al., 2001; Meier, 2002a, b; Omstedt et al., 2000; Rummukainen et al., 2001). The
75 dynamical downscaling approach utilizes regional climate models (RCMs) to refine the global climate change to
76 regional and local scales of the Baltic Sea (e.g., Rummukainen et al., 2004; Döscher et al., 2002). However,
77 these first projections were based on a single global climate model (GCM) and a single greenhouse gas (GHG)
78 concentration scenario (150% increase in equivalent CO₂ concentration in the atmosphere in future climate

¹<https://helcom.fi/helcom-at-work/events/events-2021/ccfs-launch/>



79 compared to historical climate) and only covered 10-year time slices. After these very first attempts, more
80 advanced scenario simulations using mini-ensembles (e.g., Döscher and Meier, 2004; Meier et al., 2004b; Meier
81 et al., 2004a; Räisänen et al., 2004) and centennial-long simulations were carried out (e.g., Meier, 2006; Meier et
82 al., 2006; Meier et al., 2011b) (Table 1). However, the latter studies considered only monthly mean changes of
83 the future climate compared to present climate, applying the so-called delta approach, neglecting possible
84 changes in inter-annual variability. From these oceanographic studies it was concluded that “mean annual sea
85 surface temperatures (SSTs) could increase by some 2 to 4°C by the end of the 21st century. Ice extent in the sea
86 would then decrease by some 50 to 80%. The average salinity of the Baltic Sea could range between present day
87 values and decreases of as much as 45%. However, it should be noted that these oceanographic findings, with the
88 exception of salinity, are based upon only four regional scenario simulations using two emissions scenarios and
89 two global models” (BACC Author Team, 2008).

90
91 For the second assessment of climate change in the Baltic Sea region (BACC II Author Team, 2015),
92 continuously integrated transient simulations from present to future climates became available, even including
93 marine biogeochemical modules (e.g., Eilola et al., 2013; Friedland et al., 2012; Gräwe and Burchard, 2012;
94 Gräwe et al., 2013; Gröger et al., 2019; Gröger et al., 2021b; Holt et al., 2016; Kuznetsov and Neumann, 2013;
95 Meier et al., 2011a; Meier et al., 2011b; Meier et al., 2012a; Meier et al., 2012c; Meier et al., 2012d; Neumann,
96 2010; Neumann et al., 2012; Omstedt et al., 2012; Pushpadas et al., 2015; Ryabchenko et al., 2016; Skogen et al.,
97 2014) and higher tropic levels (e.g., Bauer et al., 2019; Ehrnsten et al., 2020; Gogina et al., 2020; Holopainen et
98 al., 2016; MacKenzie et al., 2012; Niiranen et al., 2013; Vuorinen et al., 2015; Weigel et al., 2015). The BACC
99 II Author Team (2015) concluded that “recent studies confirm the findings of the first assessment of climate
100 change in the Baltic Sea basin”. Detailed key messages were that “No clear tendencies in saltwater transport
101 were found. However, the uncertainty in salinity projections is likely to be large due to biases in atmospheric and
102 hydrological models. Although wind speed is projected to increase over sea, especially over areas with
103 diminishing ice cover, no significant trend was found in potential energy ...” (a measure of energy to
104 homogenize the water column). “In accordance with earlier results, it was found that sea-level rise has greater
105 potential to increase surge levels in the Baltic Sea than does increased wind speed. In contrast to the first BACC
106 assessment (BACC Author Team, 2008), the findings reported in this chapter are based on multi-model
107 ensemble scenario simulations using several GHG emissions scenarios and Baltic Sea models. However, it is
108 very likely that estimates of uncertainty caused by biases in GCMs are still underestimated in most studies.”
109 (BACC II Author Team, 2015).

110
111 Since the early 21st century, transient simulations for the period 1960–2100 using regional ocean (Holt et al.,
112 2016; Pushpadas et al., 2015) and regional coupled atmosphere–ocean models, so-called Regional Climate
113 System Models (RCSMs; Bülow et al., 2014; Dieterich et al., 2019; Gröger et al., 2019; Gröger et al., 2021b)
114 have also been available for the entire, combined Baltic Sea and North Sea system. An overview was given by
115 (Schrum et al., 2016) as part of the North Sea Region Climate Change Assessment Report (NOSCCA, (Quante
116 and Colijn, 2016)) and by Gröger et al. (2021a) within the Baltic Earth Assessment Report (BEAR) project (this
117 thematic issue).

118



119 There is a notable difference in salinity projections between the first two assessments (BACC Author Team,
120 2008; BACC II Author Team, 2015) and recent scenario simulations (Meier et al., 2021). While the first Baltic
121 Sea scenario simulations driven by nine RCMs and five GCMs showed a pronounced negative ensemble mean
122 change in salinity because two of the involved GCMs showed a significant increase in the mean west wind
123 component (Meier et al., 2006), such pronounced changes in the large-scale atmospheric circulation were not
124 observed in later studies anymore (Saraiva et al., 2019a). The large spread in river discharge did not decrease
125 between the various studies ranging between -8 and +26% (Meier et al., 2006; 2021). As global sea level rise
126 projections were corrected in more recent assessments towards higher rates (e.g., IPCC, 2019a; Bamber et al.,
127 2019), recent scenario simulations for the Baltic Sea also considered sea level rise (Meier et al., 2021). As a
128 consequence of compensating effects of the competing drivers of salinity changes, i.e. wind, freshwater input
129 and sea level, future salinity changes are only small (Table 2).

130

131 The aim of this study is to provide an overview over projections performed since 2013, i.e. after the last
132 assessment of climate change for the Baltic Sea basin, and to compare recent results with previous findings by
133 the BACC II Author Team (2015). We focus on projections for the marine environment, both physics and
134 biogeochemistry. Variables such as temperature, salinity, oxygen, phosphate, nitrate, phytoplankton
135 concentration, primary production, nitrogen fixation, hypoxic area and Secchi depth (measuring water
136 transparency) are analyzed. An accompanied study by Christensen et al. (2021) investigated atmospheric
137 projections in the Baltic Sea region. For an overview on the development of RCMs and their applications the
138 reader is referred to Gröger et al. (2021a). For the comparison between the various studies of scenario
139 simulations, we analyze only published data (Table 1). We focus the analysis on two recently generated sets of
140 scenario simulations, henceforth called BalticAPP and CLIMSEA (Table 1, see Saraiva et al., 2019a, b; Meier et
141 al., 2019a; 2021), that we compare with the previous, henceforth called ECOSUPPORT scenario simulations
142 (Meier et al., 2014), which were assessed by the BACC II Author Team (2015). Efforts of investigating the
143 impact of climate change on the Baltic Sea primary production without utilizing a regional climate model (Holt
144 et al., 2016; Pushpadas et al., 2015) are not addressed in this study. Also nutrient input reduction scenarios under
145 present climate, e.g. described by Friedland et al. (2021), are not considered. To our knowledge, further
146 coordinated experiments of projections for the coupled physical-biogeochemical system of the Baltic Sea after
147 2013 were not published. Uncoordinated scenario simulations performed prior to 2013 (including Ryabchenko et
148 al., 2016) and their uncertainties were previously discussed by Meier et al. (2018a; 2019b).

149

150 The paper is organized as follows. In Section 2, the dynamical downscaling method, the catchment and Baltic
151 Sea models, the experimental setup and the analysis strategy are introduced. In Section 3, for historical and
152 future climates results of the three sets of scenario simulations, ECOSUPPORT, BalticAPP and CLIMSEA, are
153 compared. Knowledge gaps and a summary finalize the study.



154 2 Methods

155 2.1 Regionalization of changing climate

156 Dieterich et al. (2019) produced an ensemble of scenario simulation with a coupled RCSM, called RCA4-
157 NEMO. RCA4-NEMO was introduced by Wang et al. (2015). Gröger et al. (2019; 2021b), and Dieterich et al.
158 (2019) have validated and analyzed different aspects of the RCA4-NEMO ensemble discussed here. The
159 atmospheric component RCA4 was run at a resolution of 0.22 degrees and 40 levels in the EURO-CORDEX
160 domain (Jacob et al., 2014). Coupled to it is the North Sea-Baltic Sea model NEMO at a resolution of two
161 nautical miles (3.7 km) and 56 levels. The two components of the RCSM are coupled by sending sea level
162 pressure, energy, mass and momentum fluxes every three hours from the atmosphere to the ocean. Vice versa,
163 the atmosphere receives at the same frequency sea and ice surface temperatures and the sea-ice fraction and
164 albedo.

165

166 This RCSM has been applied to downscale eight different Earth System Models (ESMs) driven by three
167 Representative Concentration Pathways (RCPs) each. For the Baltic Sea projections, four ESMs (MPI-ESM-LR,
168 EC-Earth, IPSL-CM5A-MR, HadGEM2-ES; see Gröger et al. (2019) with references for the ESMs therein) and
169 the GHG concentration scenarios RCP4.5 and RCP8.5 were selected (Table 3). The four ESMs were part of the
170 Fifth Coupled Model Intercomparison Project (CMIP5; Taylor et al., 2012) and their results were assessed by the
171 Fifth IPCC Assessment Report (AR5; IPCC, 2013).

172

173 Surface variables of the atmospheric component were saved at hourly to 6-hourly frequency to allow for an
174 analysis of means and extremes in present and future climates. As RCA4-NEMO does not contain model
175 components for the terrestrial and marine biogeochemistry, two additional models forced with the atmospheric
176 surface fields of RCA4-NEMO, i.e. a catchment and a marine ecosystem model, were employed (Fig. 2).

177

178 For the ECOSUPPORT scenario simulations, the dynamical downscaling was performed with the regional
179 Rossby Centre Atmosphere Ocean (RCOA) model (Döscher et al., 2002). RCOA consists of the atmospheric
180 component RCA3 (Samuelsson et al., 2011) and the oceanic component RCO (Meier et al., 2003; Meier, 2007)
181 with horizontal grid resolutions of 25 km and six nautical miles (11.1 km), respectively. In the vertical, the ocean
182 model had 41 levels with varying layer thicknesses between 3 m close to the surface and 12 m at 250 m depth.
183 The latter was the maximum depth in the model.

184 2.2 Catchment model

185 The catchment model E-HYPE (Hydrological Predictions for the Environment, <http://hypeweb.smhi.se>), a
186 process-based, high-resolution multi-basin model applied for Europe (Hundecha et al., 2016; Donnelly et al.,
187 2017), and a statistical hydrological model (Meier et al., 2012c) were applied to calculate river runoff and
188 nutrient inputs under changing climate but without considering land surface changes. While the statistical model
189 calculates river runoff from precipitation minus evaporation over the catchment area, riverborne nutrient inputs
190 were estimated from the product of a given nutrient concentration and the statistically derived volume flow
191 (Gustafsson et al., 2011; Meier et al., 2012c).



192

193 In CLIMSEA, two nutrient input scenarios, defining plausible future pathways of nutrient inputs from rivers,
194 point sources and atmospheric deposition, i.e. the BSAP and reference (REF) scenarios (Saraiva et al., 2019a; b)
195 were used (Fig. 3). In BalticAPP, nutrient input scenarios followed BSAP, REF and worst (WORST) scenarios
196 (Saraiva et al., 2019a; b; Pihlainen et al., 2020). Finally in ECOSUPPORT, instead of WORST a business-as-
197 usual (BAU) scenario was applied (Gustafsson et al., 2011; Meier et al., 2011a). In the BSAP scenario in
198 CLIMSEA and BalticAPP, nutrient inputs linearly decrease from current values in 2012 (i.e., the average for
199 2010–2012) to the maximum allowable input in 2020, defined by the mitigation plan. After that, the nutrient
200 inputs remain constant until the end of the century. A similar temporal evolution was defined in ECOSUPPORT
201 but with a reference period 1997-2003 (Gustafsson et al., 2011; their Fig. 3.1). In the REF scenario, in
202 CLIMSEA and BalticAPP, the nutrient inputs were calculated by E-HYPE that considered the impact of
203 changing river flow on nutrient inputs but that neglected any changes in land use or socioeconomic development.
204 These inputs correspond approximately to the observed inputs during the period 2010-2012. The two additional,
205 above-mentioned scenarios on future projections, BAU and WORST, cannot be compared because the
206 corresponding input assumptions differ (see Meier et al., 2018a). However, both are characterized by population
207 growth and intensified agricultural practices such as land cover changes and fertilizer use (HELCOM, 2007;
208 Zandersen et al., 2019; Pihlainen et al., 2020) and are only discussed in this study for the sake of completeness.

209 **2.3 Baltic Sea model**

210 The coupled physical-biogeochemical ocean model (RCO-SCOB) was driven by the atmospheric surface field
211 data calculated by RCA4-NEMO and by the river runoff and nutrient input scenarios derived from E-HYPE
212 projections and atmospheric deposition (Fig. 2). Atmospheric depositions were assumed to be constant at the
213 observed levels during 2010-2012 or reduced as in the BSAP. RCO is a Bryan-Cox-Semtner-type ocean
214 circulation model with horizontal and vertical grid resolutions of 3.6 km and 3 m, respectively (Meier et al.,
215 1999; 2003; Meier, 2001; 2007). SCOB is a biogeochemical module of the nutrient-phytoplankton-zooplankton-
216 detritus (NPZD) type, considering state variables such as phosphate, nitrate, ammonium, oxygen concentration,
217 phytoplankton concentrations of three algal types (diatoms, flagellates and others, cyanobacteria) and detritus
218 (Eilola et al., 2009; Almroth-Rosell et al., 2011; 2015). RCO-SCOB was used in many Baltic Sea climate
219 applications (for an overview see Meier and Saraiva, 2020), evaluated with respect to measurements and
220 compared with other Baltic Sea models (Eilola et al., 2011; Placke et al., 2018; Meier et al., 2018a).

221 **2.4 Scenario simulations**

222 In CLIMSEA, we have analysed an ensemble of 48 RCO-SCOB scenario simulations for the period 1976-2098
223 (Table 3) that was produced following the dynamical downscaling approach described in the Sections 2.1 to 2.3
224 (Fig. 2) and presented by Meier et al. (2021). Contrary to previous studies (Meier et al., 2011a; Saraiva et al.,
225 2019a), the CLIMSEA scenario simulations also consider various scenarios of global sea level rise (SLR). Meier
226 et al. (2021) applied three SLR scenarios starting from the year 2005. In these scenarios, by the year 2100 the
227 projected mean sea level changes relative to the seabed are: (scenario 1) 0 m, (scenario 2) the ensemble mean of
228 RCP4.5 (0.54 m) and RCP8.5 (0.90 m) IPCC projections (IPCC, 2019b; Hieronymus and Kalén, 2020) and
229 (scenario 3) the 95th percentiles of the low- (1.26 m, here combined with RCP4.5) and high-case (2.34 m, here



230 combined with RCP8.5) scenarios following Bamber et al. (2019) (Table 3). By deepening the water depth at all
231 grid points every 10 years the relative sea level linearly increased. The spatially varying land uplift was not
232 considered. For details, the reader is referred to (Meier et al., 2021).

233

234 The CLIMSEA ensemble simulations were compared with earlier ensemble scenario simulations by Meier et al.
235 (2011a; 2012c) and Neumann et al. (2012), called ECOSUPPORT, and by Saraiva et al. (2019a, b) and Meier et
236 al. (2019a), called BalticAPP. Both sets of scenario simulations, ECOSUPPORT and BalticAPP, applied a
237 similar downscaling approach as used for the CLIMSEA projections (Fig. 2). However, the scenario simulations
238 of ECOSUPPORT were based upon different global and regional climate models, three coupled physical-
239 biogeochemical models for the Baltic Sea and previous GHG emission scenarios as detailed by the Fourth IPCC
240 Assessment Report (AR4) (Table 1). Compared to BalticAPP, the CLIMSEA ensemble was enlarged by three
241 SLR scenarios (Table 3) whereas previous projections assumed that the mean sea level relative to the seabed will
242 not change. The need for including SLR scenarios is based upon the finding that the relative sea level above the
243 sills in the entrance area limits the transport and controls salinity in the entire Baltic Sea (Meier et al., 2017). As
244 the relative SLR during the period 1915–2014 was estimated to be 0–1 mm year⁻¹, resulting from the net effect
245 of past eustatic SLR and land uplift (Madsen et al., 2019), an optimistic scenario for the future would be an
246 unchanged relative water level above the sills (Meier et al., 2021). In CLIMSEA, mean and high-case scenarios
247 follow the median values of RCP4.5 and RCP8.5 ensembles by (Oppenheimer et al., 2019) and the 95th
248 percentiles of low- and high-case scenarios by Bamber et al. (2019) (Table 3).

249 **2.5 Analysis**

250 *Evaluation of the historical period*

251 To evaluate model results of the BalticAPP and CLIMSEA scenario simulations during the historical period,
252 annual and seasonal mean biases during the historical period between RCO-SCOBIs simulations and reanalysis
253 data (Liu et al., 2017) were calculated. As the reanalysis data are available for the period 1971-1999, we limit the
254 calculation of biases to 1976-1999. Model data of historical periods of BalticAPP and ECOSUPPORT scenario
255 simulations were evaluated by Saraiva et al. (2019a, b) and Meier et al. (2011a; 2012c, d), respectively.

256

257 *Mixed layer depth*

258 The mixed layer depth (MLD) was calculated following de Boyer Montégut et al. (2004).

259

260 *Secchi depth*

261 Secchi depth (S_d) is a measure of water transparency and is calculated from $S_d = 1.7/k(\text{PAR})$, where $k(\text{PAR})$ is
262 the coefficient of underwater attenuation of the photosynthetically available radiation (Kratzer et al., 2003).
263 Factors controlling $k(\text{PAR})$ in the RCO-SCOBIs model were the concentrations of phytoplankton and detritus. In
264 addition, salinity was used in one of the other Baltic Sea models (ERGOM) of the ECOSUPPORT ensemble as a
265 proxy of the spatio-temporal dynamics of yellow substances.

266

267 *Trends*



268 First, the monthly average of SST was computed from model output every 48 hours. Then the linear trend was
269 calculated with the Theil-Sen estimator (Theil, 1950; Sen, 1968). The trend computed with this method is the
270 median of the slopes determined by all pairs of sample points. The advantage of this expensive method is that it
271 is much less sensitive to outliers. The significance of SST trends was evaluated from a Mann-Kendall non-
272 parametric test with a threshold of 95%. The SST trends were computed by season and annually. In this last case
273 the annual cycle is removed before computing the linear trend.

274

275 Following Kniebusch et al. (2019), a ranking analysis was performed to determine, which atmospheric drivers
276 others than air temperature are most important for the monthly variability of SST in each ESM forcing of the
277 CLIMSEA data set and in both RCP scenarios, RCP4.5 and RCP8.5. The SST trend is dominated by the trend in
278 air temperature, thus to partly cancel the air temperature effect on SST, the residuals from a linear model fitting
279 the SST to the surface atmosphere temperature (SAT) was subtracted from the SST. Then a cross-correlation
280 analysis was applied to determine the main factor driving the SST trend. For each grid point and variable (i.e.
281 cloudiness, latent heat flux, and u-v wind components), the explained variance was calculated and the variable
282 explaining the most variance was identified.

283

284 *Marine heat waves*

285 During the past decades, the Baltic Sea region warmed up faster than the global mean warming (Rutgersson et
286 al., 2015; Kniebusch et al., 2019) and any other coastal sea (Belkin, 2009) making this region prone to marine
287 heat waves (MHWs). Short periods of abnormally high water temperatures have recently been documented for
288 the Baltic Sea (Suursaar, 2020). MHWs can be defined with reference to the mean climatology (e.g. 90th, 95th,
289 98th percentile temperature) or by exceeding absolute temperature thresholds to be defined with respect to end
290 user applications (Hobday et al., 2018). In most cases, MHWs are defined by the number of periods, the
291 intensity, and duration and for specific purposes (Hobday et al., 2018). We here only focus on the general impact
292 of climate change since an appropriate definition of metrics for MHWs suitable for the Baltic is lacking. In the
293 following, MHWs are defined as periods with an SST $\geq 20^{\circ}\text{C}$ lasting for at least 10 days to better reflect the
294 sensitivity of ecosystem dynamics.

295 **3 Results**

296 **3.1 Historical period**

297 **3.1.1 Water temperature**

298 The climate of the Baltic Sea region varies considerably due to maritime and continental weather regimes. For
299 the period 1970 to 1999, the annual mean SST amounts to about 7.8°C (Fig. 4). The mean seasonal cycle of the
300 SST is pronounced and the northern Baltic Sea is sea-ice covered every winter (not shown). Due to the large
301 latitudinal extension, the Baltic Sea is characterized during all seasons by a distinct SST difference between
302 colder northern and warmer southern sub-basins (Fig. 4). In the southern Baltic Sea, there is also a pronounced
303 west-east temperature gradient, mainly during summer and autumn, which reflects the large-scale cyclonic



304 circulation that advects warmer and more saline southern waters along the eastern coast and colder less saline
305 waters of northern origin at the western side (see Gröger et al., 2019, their Suppl. Mat. S1; Fig. 4).

306

307 On average, during the historical period 1976-2005 CLIMSEA climate simulations are warmer compared to the
308 reanalysis data (Fig. 4). In particular, during spring and summer, the shallow coastal zone of the northern and
309 eastern Baltic Sea is too warm. The spatially averaged biases during winter, spring, summer, autumn and the
310 annual mean amount to 0.8, 0.9, 0.8, 1.0 and 0.9°C. The reason for the warm bias is likely a bias of the RCM.
311 Driven by the reanalysis data ERA40 (Uppala et al., 2005), RCA4-NEMO systematically overestimates water
312 temperatures and underestimates sea-ice cover in the Baltic Sea during the historical period (Gröger et al., 2019;
313 their Suppl. Mat. S1).

314

315 In ECOSUPPORT scenario simulations, there is also a systematic warm bias of RCAO driven by GCMs at the
316 lateral boundaries, particularly resulting in too warm winter water temperatures and too low sea-ice cover (Meier
317 et al., 2011c, d; 2012c, d). While these biases are found in all three applied Baltic Sea models (Table 3) forced
318 with the RCM atmospheric surface fields, simulations driven with regionalized reanalysis data (ERA40)
319 showed smaller mean biases (Eilola et al., 2011).

320 3.1.2 Mixed layer depth

321 Figure 5 shows the seasonal MLD cycle calculated after de Boyer Montégut et al. (2004). A deeper MLD is seen
322 over the open ocean with pronounced west - east gradients. This is related to the predominant south-westerly
323 wind regime with larger wind fetches and higher significant wave heights in the eastern Gotland Basin causing
324 wave-induced vertical mixing. Furthermore, a positive sea - atmosphere temperature contrast favors higher wind
325 speeds ("positive winter thermal feedback loop"; Gröger et al., 2015; 2021b). In spring, a weakening wind
326 regime, lowering heat exchange (thereby turning from heat loss to heat gain) and increased solar irradiance lead
327 to a thinner MLD in the southern Baltic Sea while in the northern part melting sea ice and subsequent thermal
328 convection and wind-induced mixing still maintain MLDs > 50 m. During summer, the atmosphere-ocean
329 dynamics is weakest leading to a pronounced thermocline and shallowest MLDs (the so-called "summer thermal
330 short circuit"; Gröger et al., 2021b). During autumn, the atmosphere cools faster than the earth surface and
331 landmasses cool faster than the open sea areas. Because of the increased thermal contrasts, the large-scale wind
332 regime strengthens with positive feedback on MLD.

333

334 The ensemble model mean in CLIMSEA reproduces this dynamics and the spatial pattern relatively well. During
335 the cold season, however, MLD is somewhat smaller than in the reanalysis data by Liu et al. (2017). This may be
336 the result of the air-sea coupling. Gröger et al. (2015, 2021b) have demonstrated that standalone ocean models
337 do not very well represent the complex thermal air -sea feedbacks in winter as fully coupled ocean-atmosphere
338 GCMs. This can result in SST biases and a too shallow MLD (Gröger et al., 2015; Figure 7a therein; Gröger et
339 al., 2021b). However, causes of the underestimated winter MLD are unknown.

340

341 In the literature, MLDs in ECOSUPPORT scenario simulations have not been analyzed.



342 **3.1.3 Marine heat waves**

343 Baltic Sea MHWs are here defined as periods of >10 days duration with 1) SST higher than 20°C and 2) SST
344 exceeding the 95th percentile temperature. Figure 6 compares the CLIMSEA climate model ensemble mean with
345 the reanalysis data set generated by the same model (Liu et al., 2017).

346

347 The first index uses a fixed threshold focusing more on the environmental impact of heat waves. In particular,
348 diazotrophic nitrogen fixation becomes effective at higher temperatures. The spatial pattern of such MHWs is
349 strongly related to the simulated SST. Figure 6a shows that such periods are mostly absent in the open sea of the
350 Baltic proper and further north in the Gulf of Bothnia. MHWs are most abundant in shallow marginal bays like
351 the Gulf of Finland and Gulf of Riga as well as along the coasts. The RCO ensemble mean produces generally
352 more frequent MHWs and MHWs of longer duration than the reanalysis data set. Furthermore, the coastal
353 signature of high abundance extends more offshore (Fig. 6a). In case of the Belt Sea and Bay of Lübeck, this
354 leads to considerable deviations from the reanalysis data set.

355

356 The second index is based on a reference climatology, which is taken here as 1976-1999. The number of MHWs
357 (Fig. 6c) is negatively correlated to their average duration (Fig. 6d). This is somewhat more pronounced in the
358 reanalysis data set. In general, reanalysis data and RCO show similar patterns but the amplitude of spatial
359 variance is higher in the reanalysis data (Fig. 6c) which assimilated small-scale regional observations. The
360 duration of MHWs in RCO (Fig. 6d) is highest in the open sea where wind events are probably the main process
361 interrupting heat waves by induced vertical mixing.

362

363 Since MHWs are predominantly a summer phenomenon in the Baltic Sea, the stability of the seasonal
364 thermocline is likely a key element in the dynamics of MHWs and processes favoring vertical mixing can be
365 considered a benchmark in the models ability to simulate MHW. Taking into account that mixing is highly
366 parameterized in current ocean models, RCO reproduces the spatial pattern of MHW reasonably well.

367

368 In the literature, MHWs in ECOSUPPORT scenario simulations have not been analyzed.

369 **3.1.4 Salinity**

370 The annual mean sea surface salinity (SSS) distribution shows a large north–south gradient mirroring the input
371 of freshwater from rivers, mostly located in the northern catchment area, and saltwater inflows from the North
372 Sea (Fig. 7). The SSS drops from about 20 g kg⁻¹ in Kattegat to < 2 g kg⁻¹ in the northern Bothnian Bay and
373 eastern Gulf of Finland. For the period 1970 to 1999, the annual mean SSS of the Baltic Sea including Kattegat
374 amounts to about 7.3 g kg⁻¹. Occasionally big inflows of heavy saltwater from Kattegat ventilate the bottom
375 water of the Baltic Sea, filling its deeper regions (Fig. 7). Due to almost absent tides, mixing is limited and the
376 water column is characterized by a pronounced vertical gradient in salinity, and consequently also in density,
377 between the sea surface and the bottom.

378

379 Probably due to differences in the hydrological model (E-HYPE) data compared to observations, in the
380 CLIMSEA climate models SSS in the coastal zone and in Kattegat is on average lower compared to the



381 reanalysis data (Fig. 7). The spatially averaged, annual mean bias amounts to -0.4 g kg^{-1} . In the climate models,
382 bottom salinities in the Belt Sea, Great Belt area and the Gotland Basin (most pronounced in the northwestern
383 part) are considerably higher and in the Bornholm Basin considerably lower than in the reanalysis data (Fig. 7).
384 The spatially averaged, annual mean bias amounts to $+0.3 \text{ g kg}^{-1}$. Hence, the vertical stratification in the Belt
385 Sea, Great Belt area and the Gotland Basin is larger in climate models than in the reanalysis data.

386

387 In ECOSUPPORT scenario simulations, in the entire Baltic Sea SSS was overestimated, in particular in the
388 northern and eastern Baltic Sea (Meier et al., 2011b; 2012c). In the northern and eastern Baltic Sea, also the
389 ensemble mean bottom salinity and vertical stratification were overestimated while bottom salinity in the eastern
390 Gotland Basin was well simulated (Meier et al., 2012c).

391 3.1.5 Sea level

392 Due to the seasonal cycle in wind speed, with wind directions predominantly from southwest, the sea level in the
393 Baltic Sea varies considerably throughout the year, with highest sea levels of about 40 cm relative to Kattegat
394 during winter, at the northern coasts in the Bothnian Bay and at the eastern coasts in the Gulf of Finland (Fig. 7).
395 For the period 1976 to 1999, the annual mean sea level amounts to about 16 cm, with a horizontal north–south
396 difference of about 35 cm (not shown). This sea level slope is explained by the lighter brackish water in the
397 northeastern Baltic Sea compared to the Kattegat and by the mean wind from southwesterly directions which
398 pushes the water to the north and to the east (Meier et al., 2004a).

399

400 Differences in mean sea level between CLIMSEA climate models and reanalysis data are small (Fig. 7) and the
401 spatially averaged, winter mean bias amounts to $+0.6 \text{ cm}$ only. Sea levels in some parts of the coastal zone such
402 as the western Bothnian Sea are higher in climate models compared to the reanalysis data probably due to lower
403 salinities. The negative sea level bias in the eastern Gotland Basin suggests an intensified, basin-wide cyclonic
404 gyre. The seasonal cycle of the ensemble mean sea level is relatively well simulated, with overestimated sea
405 level in early spring and underestimated sea level in summer at all investigated tide gauge locations compared to
406 both observations and a hindcast simulation driven by regionalized ERA40 data (Fig. 8).

407

408 In ECOSUPPORT scenario simulations, sea levels were not systematically analyzed. In one of the three models
409 (RCO-SCOB1), seasonal mean biases comparable to the biases in CLIMSEA scenario simulations were found
410 (Meier et al., 2011d).

411 3.1.6 Oxygen concentration and hypoxic area

412 Since the 1940s, nutrient inputs into the Baltic Sea have increased due to population growth and intensified
413 fertilizer use in agriculture (Gustafsson et al., 2012; Fig. 3). Nutrient inputs reached their peak in the 1980s and
414 declined thereafter until the early 21st century as a consequence of the implementation of nutrient input
415 abatement strategies. Since the 1960s, the bottom water of the Baltic Sea below the permanent halocline is
416 characterized by oxygen depletion and large-scale hypoxia (Figs. 9 and 22).

417



418 Following stratification biases in the deeper sub-basins of the Baltic Sea, summer bottom oxygen concentrations
419 in the Bornholm and Gotland basins in CLIMSEA/BalticAPP climate simulations are higher and lower,
420 respectively, compared to the reanalysis data (Fig. 9). Hence, stronger vertical stratification hampers vertical
421 fluxes of oxygen causing prolonged residence times and lower bottom oxygen concentrations, especially at the
422 halocline depth of the Gotland Basin. Spatially averaged biases during winter, spring, summer, autumn and the
423 annual mean are small but systematic and amount to -0.6, -0.7, -0.7, -0.5 and -0.6 mL L⁻¹.

424

425 In ECOSUPPORT scenarios, the ensemble mean deep water oxygen concentrations in the eastern Gotland Basin
426 and in the Gulf of Finland were slightly higher (but within the range of natural variability) and significantly
427 lower compared to observations, respectively (Meier et al., 2011a; 2012d).

428 3.1.7 Nutrient concentrations

429 Nutrients (i.e., phosphorus and nitrogen) in the surface layer during winter are a good indicator for the intensity
430 of the following spring bloom. Highest sea surface concentrations of winter mean phosphate and nitrate are
431 found in the coastal zone, in particular close to the mouths of the large rivers in the southern Baltic Sea that
432 transport elevated inputs of nutrients into the sea (Fig. 9).

433

434 During the historical period 1976-1999, winter surface phosphate concentrations in climate simulations are
435 relatively close to reanalysis data (Fig. 9). Different concentrations are only found in coastal regions influenced
436 by large rivers probably due to differing inputs. Such regions are, for instance, the coastal zones affected by the
437 discharges of the Odra, Vistula and Pärnu rivers. Spatially averaged biases are largest during summer and
438 autumn and amounted to +0.2 mmol P m⁻³ in summer.

439

440 Similarly, simulated winter surface nitrate concentrations are close to reanalysis data but differed in coastal
441 regions due to different inputs from large rivers (Fig. 9). In particular, larger differences are found in the Gulf of
442 Riga and in the eastern Gulf of Finland influenced by the Neva River. Spatially averaged biases during winter,
443 spring, summer, autumn and the annual mean are rather small but systematic and amount to -1.1, -1.3, -0.5, -0.7
444 and -0.9 mmol N m⁻³.

445

446 In ECOSUPPORT scenario simulations, simulated profiles of phosphate, nitrate and ammonium were within the
447 range of observations during 1978-2007, except for phosphate in the Gulf of Finland (Meier et al., 2012d).
448 According to hindcast simulations coupled physical-biogeochemical models for the Baltic Sea showed larger
449 biases relative to the standard deviations of observations in the northern Baltic Sea than in the Baltic proper
450 (Eilola et al., 2011).

451 3.1.8 Phytoplankton concentrations

452 During the period 1976 to 1999, high concentrations of phytoplankton blooms were confined to the coastal zone,
453 the area with the highest nutrient concentrations (Fig. 10). Water transparency, measured by Secchi depth, is low
454 in the Baltic Sea compared to the open ocean (Fleming-Lehtinen and Laamanen, 2012). For the period 1970 to
455 1999, the annual mean Secchi depth averaged for the entire Baltic Sea, including Kattegat, amounts to about 6.6



456 m only. In the coastal zone, the Secchi depth is much smaller than in the open Baltic Sea (Fig. 10). Also in the
457 northern Baltic Sea, Secchi depth is smaller than in the Gotland Basin due to yellow substances originating from
458 land (Fleming-Lehtinen and Laamanen, 2012).

459

460 Following nutrient concentration biases, simulated annual mean surface phytoplankton concentrations are close
461 to reanalysis data but deviated in coastal regions (Fig. 10). Spatially averaged biases during winter, spring,
462 summer, autumn and the annual mean are rather small and amount to +0.02, -0.1, -0.009, +0.06 and -0.008 mg
463 Chl m⁻³.

464

465 Similar results are also found for the mean biases of simulated Secchi depths (Fig. 10). Furthermore, Secchi
466 depths in climate simulations are systematically deeper in the regions south of Gotland island and in the entrance
467 to the Gulf of Finland (northeastern Gotland Basin). Spatially averaged biases during winter, spring, summer,
468 autumn and the annual mean amount to +0.2, +0.4, +0.06, +0.1 and +0.2 m.

469

470 Compared to Secchi depth data from HELCOM (HELCOM, 2013; their Table 4.3) and (Savchuk et al., 2006;
471 their Table 3) the CLIMSEA climate simulations under- and overestimate Secchi depth in the southwestern and
472 northern Baltic Sea, respectively, while in the Gotland Basin model results fit observations well (Meier et al.,
473 2019a).

474

475 In ECOSUPPORT scenario simulations, Secchi depth has not been analyzed relative to observations.

476 **3.1.9 Biogeochemical fluxes**

477 An evaluation of biogeochemical fluxes such as primary production and nitrogen fixation is difficult because of
478 lacking observations. An exception is the study by Hieronymus et al., (2021) who compared historical
479 simulations with RCO-SCOBI including a cyanobacteria life cycle (CLC) model (Hense and Beckmann, 2006;
480 2010) driven by reconstructed atmospheric and hydrological data with in situ observations of nitrogen
481 fixation. Hieronymus et al. (2021) found a satisfactory agreement, mainly within the uncertainty range of the
482 observations. However, simulated monthly mean nitrogen fixation during 1999-2008 showed a prolonged peak
483 period in July and August while the observations showed a peak more confined to July. However, it should be
484 noted that the RCO-SCOBI version that has been used for scenario simulations discussed here (e.g., Saraiva et
485 al., 2019a) did not contain a CLC model.

486 **3.2 Future period**

487 **3.2.1 Water temperature**

488 *Annual and seasonal mean changes*

489 In Figs. 11 and 12, annual and seasonal mean SST changes between 1976-2005 and 2069-2098 in RCO-SCOBI
490 are depicted. The maximum seasonal warming signal propagates between winter and summer from the Gulf of
491 Finland via the Bohnian Sea into the Bothnian Bay (Fig. 11). Maximum warming occurs during summer in the
492 Bothnian Sea and Bothnian Bay. Comparing RCP4.5 and RCP8.5, seasonal patterns are similar although the



493 warming is greater in RCP8.5 compared to RCP4.5. The SLR has almost no impact on SST changes. Hence,
494 BalticAPP and CLIMSEA scenario simulation results are similar (not shown). The warming in ECOSUPPORT
495 is in between the CLIMSEA/BalticAPP RCP4.5 and RCP8.5 results because the GHG emissions of the A1B
496 scenario, which forces the ECOSUPPORT ensemble², are in between the RCP4.5 and RCP8.5 scenarios.

497

498 In the CLIMSEA/BalticAPP RCSM projections, annual mean SST changes in the Baltic Sea driven by four
499 ESMs, i.e. MPI-ESM-LR, EC-EARTH, IPSL-CMA-MR, HadGEM2-ES, under the RCP8.5 scenario amount to
500 +2.27, +3.70, +3.52 and +4.67°C (Gröger et al., 2019). Thus, the ensemble mean change is 3.54°C. The
501 corresponding ensemble mean change in RCO-SCOBI scenario simulations is smaller and amount to +2.92°C.
502 Different MLDs, vertical stratification and sea-ice cover in the two ocean models, RCO-SCOBI and NEMO,
503 may explain the different responses. Indeed, the comparison of the MLD between the two models reveals a
504 systematic shallower MLD in the RCSM compared to RCO-SCOBI (not shown), which would argue for a higher
505 sensitivity of the RCSM to climate warming.

506

507 Spatial patterns of SST changes in ECOSUPPORT (e.g., Meier et al., 2012c) and CLIMSEA (e.g., Saraiva et al.,
508 2019b) scenario simulations are similar. However, uncertainties due to the applied global (Meier et al., 2011d) or
509 regional (Meier et al., 2012b) model might be considerable. In particular, the summer ensemble range caused by
510 various GCMs is significant (Meier et al., 2011d). The differences in magnitude of the warming are explained by
511 the various GHG concentration scenarios (Fig. 12).

512

513 *Trends*

514 Since SLR and nutrient input scenarios have a negligible impact on SST changes, only a comparison between
515 RCP4.5 and RCP8.5 scenarios in CLIMSEA/BalticAPP has been done. The multi-model mean of annual SST
516 trends is about 0.18 K decade⁻¹ and 0.35 K decade⁻¹ in the RCP4.5 and RCP8.5 scenarios, respectively (Fig. 13a,
517 f). At the Baltic Sea scale, seasonal SST trends from annual values vary only slightly (± 0.01 K decade⁻¹ in both
518 scenarios). However at the sub-basin scale, seasonal variations are much stronger, reaching ± 0.05 K decade⁻¹ in
519 the northern Baltic Sea, with a maximum in summer (Fig. 13). This summer maximum in the northern Baltic Sea
520 can likely be explained by the projected declining sea-ice cover in this season, as during the 1850-2008 period
521 (Kniebusch et al., 2019).

522

523 As seen in Figure 14, relative SST trends indicate that the northern Baltic Sea will warm faster than the southern
524 Baltic Sea (0.02 K decade⁻¹ and 0.04 K decade⁻¹ in the RCP4.5 and RCP8.5 scenarios, respectively) with the
525 largest trends calculated over the entire period 2006-2099 reaching ~ 0.24 K decade⁻¹ and ~ 0.45 K decade⁻¹ in
526 RCP4.5 and RCP8.5, respectively. However, a calculation of the SST trends by 30-year slice periods every 10
527 years over the entire period shows that annual SST trends are variable over time (not shown). The natural
528 variability appears to modulate these trends with successive periods of increasing and decreasing SST trends
529 with a period of about 30 years. However, in the RCP8.5 scenario, SST trends gradually increase over the first
530 50 years of the period reaching a maximum of 0.5 K decade⁻¹ over the period 2046-2075, before declining

²One of the scenario simulations of ECOSUPPORT was driven by the generally warmer A2 scenario due to higher GHG emissions compared to A1B. However, this simulation of the ECHAM5 – MPIOM GCM is exceptional and at the end of the 21st century not much warmer than the corresponding run with the same model under the A1B scenario.



531 slightly from 2060 onwards, as in the RCP4.5 scenario, a result of the pronounced natural variability in this
532 scenario as well. Despite the robustness of the SST trends spatial pattern (p-value <0.05 everywhere), the
533 analysis of SST trends for the four ESM forcings reveals an important dependency of SST trends to atmospheric
534 forcings with a spread of ± 0.06 K decade⁻¹ from the multi-model mean in both scenarios (not shown).

535

536 At annual timescale, it is well-known that the variability of air temperature, through the sensible heat fluxes, is
537 the main driver of Baltic Sea SST (Kniebusch et al., 2019), as illustrated here by the high variance explained
538 between these two variables (between 0.85 and 0.95, Fig. 15). The minimum of variance explained is located in
539 the Bothnian Bay, where the sea ice cover isolates seawater from the air in winter.

540

541 To analyze the processes responsible for SST trends, a rank analysis from atmospheric variables (i.e. latent heat
542 fluxes, cloud cover, and u-v wind components) was performed following Kniebusch et al. (2019; Fig. 16). The
543 second parameter (after SAT) explaining the variability of SST differs according to the location and ESM.
544 Nevertheless, in all ESMs and in both RCP scenarios, zonal and meridional wind components are the variables
545 most correlated with SST along most of the coastal areas, probably because of upwelling. In the open sea of the
546 Baltic proper and Bothnian Bay, the second most important variable is cloudiness. This is also the case in the
547 Bothian Sea under the RCP4.5 scenario. However, in the RCP8.5 the second most important variable is at this
548 location the latent heat flux. The difference might be explained by the complete melting of the sea ice under
549 RCP8.5, amplifying air-sea exchange.

550

551 In the vertical, temperature trends are largest in the surface layer compared to the Baltic Sea winter water above
552 the halocline causing a more intense seasonal thermocline (see Section 3.2.2) with largest trends in spring and
553 summer (not shown). Elevated trends are also found in the deep water due to the influence of saltwater inflows
554 that will be warmer in future climate because the inflows originate from the shallow entrance area mainly in
555 winter. Hence, the deep water below the halocline in those sub-basins that are sporadically ventilated by lateral
556 saltwater inflows such as the Bornholm Basin and the Gotland Basin warm more than the overlying
557 intermediate layer water.

558

559 In the literature, trends in ECOSUPPORT scenario simulations were not analyzed.

560 **3.2.2 Mixed layer depth**

561 In Figure 17, changes in MLD are shown. During winter reduced sea ice cover favors a widespread deepening of
562 the MLD in the Bothnian Sea and Bothnian Bay likely caused by wind-induced mixing. In spring, the most
563 pronounced feature is a strong shallowing of MLD in the Bothnian Sea likely caused by the radiative fluxes that
564 warm the surface layer and less thermal convection (Hordoir and Meier, 2012). During the historical period,
565 water temperatures are between 2.0 and 3.0 °C in this area (Fig. 4) so warming between 1.6 and 2.4 °C (Fig. 11)
566 may hamper thermal convective mixing in future.

567

568 Changes during summer are less pronounced. Contrary to winter, an overall shallowing is found. This is in
569 agreement with a shallower and more intense thermocline in warming scenarios as suggested by Gröger et al.



570 (2019) and a common feature among projections because changes in wind speed are small (Christensen et al.,
571 2021). The autumn is primarily characterized by a prolongation of the thermal stratification leading to an overall
572 shallower MLD compared to the historical period.

573

574 It was speculated that these changes in thermocline depth during summer might have an impact on the vertical
575 overturning circulation (Hordoir et al., 2018; 2019). However, the meridional overturning circulation in the
576 Baltic proper does not show a clear signal but a northward expansion of the main overturning cell (Gröger et al.,
577 2019). Indeed, the effect is expected to be small (Placke et al., 2021).

578 3.2.3 Marine heat waves

579 Figure 18 shows the number of MHW within climatological 30-year time slices. Under conditions of the
580 historical climate MHWs are virtually absent in open ocean areas. They are most frequent in shallow regions and
581 more abundant along the eastern compared to the western coasts, which may reflect that coastal upwelling events
582 occur more frequent along the western compared to the eastern Baltic Sea coasts. Already under the RCP4.5
583 scenario, wide areas of the Baltic proper are affected by MHWs ~ once a year. The strongest response is
584 projected for the high emission RCP8.5 scenario in marginal basins like the Gulf of Riga or the Gulf of Finland
585 where MHWs would occur 2-3 times per year in future. Not only the frequency but also the average duration of
586 MHW increase with climate warming. Under RCP8.5 even in the open Gulf of Bothnia MHWs of ~20 day
587 duration would occur in future (Fig. 18). The increase in MHWs in the Baltic Sea is likewise linked to an
588 increased frequency of tropical nights in the Baltic Sea (Meier et al., 2019a; Gröger et al., 2021b).

589

590 Another way to analyze MHWs is to calculate them with respect to the 95th percentile temperature of the
591 historical reference climate (Fig. 19). For the historical climate, such periods are in most regions less than 20-30
592 days. In the southern Baltic Sea, especially west of the Baltic proper they are more frequent. The climate change
593 signal is characterized by more frequent MHWs of longer duration. Already in RCP4.5 MHWs occur at least
594 every year. The strongest increase in frequency is near the coasts whereas their average duration increases less
595 compared to the open sea (Fig. 19). This is probably related to repeated cold water entrainments from the open
596 sea that interrupt warm periods because of the larger variability of the coastal zone compared to the open sea. In
597 addition, shallow areas are, due to their lower heat storage, more sensitive to cold weather events and the
598 associated oceanic heat loss.

599 3.2.4 Salinity

600 In the CLIMSEA ensemble, salinity changes are not robust, i.e. the ensemble spread is larger than the signal
601 (Meier et al., 2021). The ensemble mean signal is small compared to the ensemble spread because the impact of
602 the projected increase in total river runoff from the entire catchment (Fig. 3) on salinity is compensated by the
603 impact of larger saltwater inflows due to the projected SLR (not shown). The results would be about the same if
604 only the IPCC mean SLRs are considered. Hence, compared to previous studies such as those by Meier et al.
605 (2011a) (ECOSUPPORT) and Saraiva et al. (2019a) (BalticAPP) (Fig. 12), salinity changes in CLIMSEA are
606 much smaller (not shown) and it is impossible to judge whether these changes will be positive or negative.



607 **3.2.5 Sea level**

608 Following global sea level changes, SLR in the Baltic Sea will accelerate in future (Hünicke et al., 2015; Church
609 et al., 2013; Bamber et al., 2019; Oppenheimer et al., 2019; Weisse and Hünicke, 2019), albeit somewhat slower
610 than the global mean because of the remote impact of the melting Antarctic ice sheet (Grinsted, 2015). For a
611 mid-range scenario, Baltic SLR is projected to be ~87% of the global mean (Pellikka et al., 2020). Further, land
612 uplift partly compensates for the eustatic SLR, in particular in the northern Baltic Sea (e.g., Hill et al., 2010). In
613 RCP2.6 and RCP8.5, the global mean sea level in 2100 is 43 cm and 84 cm higher, respectively, compared to the
614 period 1986–2005 (Oppenheimer et al., 2019). For these two scenarios, likely ranges amount to 29–59 cm and
615 61–110 cm, respectively. Assessing the ice sheet dynamics in more detail, Bamber et al. (2019) estimated for
616 low- and high case scenarios global-median SLRs of 69 and 111 cm in 2100, respectively. They found likely
617 ranges of 49–98 cm and 79–174 cm and very likely ranges of 36–126 cm and 62–238 cm.

618

619 In BalticAPP and CLIMSEA scenario simulations, sea level changes are small (Fig. 12). On the other hand, sea
620 level changes in ECOSUPPORT scenario simulations are larger, particularly in spring, because one member of
621 the multi-model ensemble considered Archimedes' principle (not shown). Note that in Figure 12 sea level
622 changes consider only changing river runoff, changing wind, and melting sea ice affecting the sea level via
623 Archimedes' principle (only in the ECOSUPPORT ensemble) whereas the global mean SLR and land uplift are
624 not included and have to be added (e.g., Meier, 2006; Meier et al., 2004a).

625

626 In CLIMSEA, pronounced seasonal changes relative to the SLR do not exist (Fig. 20). In both GHG
627 concentration scenarios, largest changes of only about ± 5 cm were found. These results confirm that systematic
628 changes in the regional wind field are small (Christensen et al., 2021). Nonlinear effects are small as well, i.e.
629 mean sea level changes do not significantly differ between various SLR scenarios (not shown).

630

631 Due to the global mean SLR, sea level extremes in the Baltic Sea that are rare today will become more common
632 in the future (e.g., Hieronymus and Kalén, 2020). However, changes in sea level extremes relative to the mean
633 sea level are statistically not significant because wind velocities are projected to remain unchanged (Christensen
634 et al., 2021). Exceptions are areas with sea ice decline because the planetary boundary will get less stable and
635 wind speeds will increase (Meier et al., 2011b).

636

637 As sea level extremes also depend on the path of low pressure systems (Lehmann et al., 2011; Suursaar and
638 Sooäär, 2007) that do not show systematic changes in future climate (Christensen et al., 2021), changes in sea
639 level extremes are highly uncertain. In addition, a large internal variability at low frequencies prevents the
640 detection of climate warming related changes in sea level extremes (Lang and Mikolajewicz, 2019).

641 **3.2.6 Oxygen concentration and hypoxic area**

642 *Bottom oxygen concentration*

643 Projected bottom oxygen concentration changes differ considerably between ECOSUPPORT and
644 BalticAPP/CLIMSEA scenario simulations as illustrated for summer (Fig. 21) whereas the differences between
645 the BalticAPP (SLR = 0 cm) and CLIMSEA (SLR > 0 cm) scenarios are relatively smaller (Meier et al., 2021).



646 The differences between ECOSUPPORT and BalticAPP ensembles mainly reflect the different experimental
647 setups of the simulations and the different nutrient input scenarios (Meier et al., 2018a). While in the shallow
648 regions without pronounced halocline future bottom oxygen concentrations decrease in all scenario simulations
649 due to the reduced oxygen saturation concentration, in the deeper offshore regions with a halocline, changes in
650 bottom oxygen concentration depend largely on the applied nutrient input scenario (Fig. 21). In ECOSUPPORT
651 scenario simulations, future bottom oxygen concentration decreases in all scenarios significantly except under
652 BSAP where the bottom oxygen concentrations in the deeper regions only slightly change on average (cf. Meier
653 et al., 2011a). By contrast, in BalticAPP projections, bottom oxygen concentrations under BSAP increase in the
654 deeper regions considerably regardless of the degree of warming (cf. Saraiva et al., 2019a; Meier et al., 2011a).
655 Under RCP4.5, bottom oxygen concentrations increase even under REF and WORST nutrient inputs whereas
656 under RCP8.5 slight reductions in the Bothnian Sea and southwestern Baltic Sea, in particular under WORST,
657 are found. These results are explained by the historical nutrient input reductions and the slow response of the
658 Baltic Sea. Similar results are also calculated for the CLIMSEA ensemble (cf. Meier et al., 2021).

659

660 *Hypoxic area*

661 In ECOSUPPORT, hypoxic area is projected to increase under REF and BAU nutrient input scenarios (Meier et
662 al., 2011a). Only under BSAP, a slight decrease compared to the early 2000s is found.

663

664 In CLIMSEA under REF, hypoxic area is projected to slightly decrease until about 2050 as a delayed response to
665 nutrient input reductions and then to increase again towards the end of the century likely a response to nutrient
666 input increase and warming (Fig. 22). Larger hypoxic areas are calculated under RCP8.5 than under RCP4.5.
667 Under BSAP, hypoxic area is projected to considerably decrease. At the end of the century, the size of hypoxic
668 area is between 78 and 22% smaller compared to the average size of the period 1976–2005. The given range
669 denotes the results of the various ensemble members.

670 **3.2.7 Nutrient concentrations**

671 While in ECOSUPPORT scenario simulations projected winter surface phosphate concentrations increase in
672 future climate under all three nutrient input scenarios (except in the Gulf of Finland in BSAP), in BalticAPP
673 projections winter surface phosphate concentrations decrease almost everywhere (except in the Odra Bight and
674 adjacent areas in REF and WORST) (not shown). In contrast to spatial patterns of surface phosphate
675 concentration changes, larger nitrate concentration changes are usually confined to the coastal zone, showing
676 varying signs of the changes. In ECOSUPPORT projections, winter surface nitrate concentrations increase in
677 particular in the Gulf of Riga, eastern Gulf of Finland, and along the eastern coasts of the Baltic proper in REF
678 and BAU (not shown). In BalticAPP projections, in REF and WORST winter surface nitrate concentrations
679 increase in particular in Bothnian Bay and Odra Bight while concentrations decrease in the Gulf of Riga and
680 Vistula lagoon. Overall, the differences in surface nutrient concentrations between the two ensembles are
681 considerable (not shown). These differences are explained by largely differing nutrient inputs from land. While
682 in ECOSUPPORT, projected changes in inputs refer to the average inputs during 1995–2002, in BalticAPP
683 scenario simulations the observed past changes including the decline in nutrient inputs since the 1980s are
684 considered (Meier et al., 2018a).



685 **3.2.8 Phytoplankton concentrations**

686 Annual mean changes in surface phytoplankton concentration (expressed as chlorophyll concentration) follow
687 the changes in nutrient concentrations and are confined to the productive zone along the coasts (Fig. 23). In
688 ECOSUPPORT projections, annual mean Secchi depths are decreasing in all scenario simulations (see Fig. 24
689 and Table 7). On the other hand, in BalticAPP projections, area averaged Secchi depths generally increase,
690 except in the combination of RCP8.5 and BAU scenarios (Table 7), indicating an improvement of the water
691 quality in future compared to present climate. The most striking changes occur in the BSAP scenario, showing
692 Secchi depth increases of up to 2 m in the coastal zone of the eastern Baltic proper. Changes in stratification
693 (illustrated by the differences between BalticAPP and CLIMSEA ensembles and between CLIMSEA ensemble
694 mean and high SLR scenarios) have only a minor impact on the water transparency response (Table 7). The
695 overwhelming driver of Secchi depth changes are nutrient input scenarios (illustrated by the differences between
696 ECOSUPPORT and BalticAPP/CLIMSEA ensembles highlighted by even contradictory signs in the changes).

697 **3.2.9 Biogeochemical fluxes**

698 In CLIMSEA under the BSAP, primary production and nitrogen fixation were projected to considerably decrease
699 in future climate (Fig. 22). Under this scenario, the interannual variability would decline. Under REF, nitrogen
700 fixation is projected to slightly decrease until about 2050 as a delayed response to nutrient input reductions and
701 then to increase again towards the end of the century likely a response to nutrient input increase and warming. At
702 the end of the century, both primary production and nitrogen fixation would be at the same level as under current
703 conditions. The impact of warming is larger under high as under low nutrient conditions (cf. Saraiva et al.,
704 2019b).

705 **3.2.10 Relation to the large-scale atmospheric circulation**

706 The most dominant large-scale atmospheric pattern controlling the climate in the Baltic Sea region during winter
707 is the North Atlantic Oscillation (NAO; Hurrell, 1995). However, this relationship is not stationary but depends
708 on other modes of variability such as the Atlantic Multidecadal Oscillation (AMO; Börgel et al., 2020). During
709 past climate, the relationship between the NAO index and regional climate variables in the Baltic Sea region,
710 such as SST, changed over time (Vihma and Haapala, 2009; Omstedt and Chen, 2001; Hünicke and Zorita, 2006;
711 Chen and Hellström, 1999; Meier and Kauker, 2002; Beranová and Huth, 2008).

712
713 Figure 25 shows the calculated ensemble mean NAO index for the period 2006 – 2100. For the RCP4.5 emission
714 scenario, it is found that the NAO shows high interannual variability. By applying a wavelet analysis, it is found
715 that the calculated NAO index contains some decadal variability, which differs for every model (not shown). By
716 comparing RCP4.5 and the high emission scenario RCP8.5, it can be seen that the spread of the ensemble
717 increases with enlarged greenhouse gas concentrations. Furthermore, Figure 25 shows the running correlation
718 between the NAO index and the area averaged SST. Indeed, the correlation remains positive but it is not constant
719 in time. By comparing RCP4.5 and RCP8.5 it is found that there are no systematic changes between both
720 emission scenarios. However, for RCP8.5 a slightly larger ensemble spread is found.



721 **4 Knowledge gaps**

722 As in this study only four ESMs were regionalized using one RCM, the CLIMSEA ensemble is still too small
723 to estimate uncertainties caused by ESM and RCM differences. It should be noted that recently even nine
724 ESMs with the same RCM were regionalized but without running modules for the terrestrial and marine
725 biogeochemistry (Gröger et al., 2021b). Therefore, we have not considered these simulations in our assessment.

726

727 Furthermore, in this study the uncertainties related to unresolved physical and biogeochemical processes in the
728 Baltic Sea and on land were not considered because only one Baltic Sea and one catchment model were used.
729 Although the CLIMSEA ensemble is larger than the ensembles in previous studies, it is still too small to estimate
730 all sources of uncertainty.

731

732 In addition to the uncertainties related to global and regional climate and impact models, the unknown pathways
733 of GHG and nutrient emissions, the role of natural variability versus anthropogenic forcing is not well
734 understood (Meier et al., 2018a; 2019b; 2021). Recent studies suggested that the impact of natural variability
735 such as the low-frequency AMO is larger than hitherto estimated. For instance, it was shown that in paleoclimate
736 simulations the AMO affects Baltic Sea salinity on time scales of 60-180 years (Börgel et al., 2018) which is
737 longer than the simulation periods of available scenario simulations. Further, the AMO may influence also the
738 centers of action of the NAO (Börgel et al., 2020). The lateral tilting of the positions of Icelandic Low and
739 Azores High explains the correlation changes between NAO and regional variables such as water temperature,
740 sea-ice cover and river runoff in the Baltic Sea region (Börgel et al., 2020). Although there are indications that
741 the AMO is affected by various climate states such as the Medieval Climate Anomaly and the Little Ice Age
742 (Wang et al., 2017; Börgel et al., 2018), it is unknown how future warming would affect these modes of climate
743 variability.

744

745 We have not analyzed changes in sea-ice cover because in the recent scenario simulations of the CLIMSEA
746 ensemble sea-ice cover is systematically underestimated. However, we found that future sea-ice cover is
747 projected to be considerably reduced, with an on average ice-free Bothnian Sea and western Gulf of Finland.
748 Recent results by Höglund et al. (2017) confirmed earlier results by Meier (2002b) and Meier et al. (2011c;
749 2014), see BACC Author Team (2008).

750

751 Most noticeable are the differences in projected biogeochemical variables between ECOSUPPORT and
752 BalticAPP/CLIMSEA ensembles. In ECOSUPPORT, nutrient input changes relative to the historical period
753 1961-2006 with prescribed observed nutrient inputs from the period 1995-2002 were applied (Gustafsson et al.,
754 2011; Meier et al., 2011a). During the historical period 1980-2002, these inputs were lower than in
755 BalticAPP/CLIMSEA scenario simulations because in the latter the observed monthly nutrient inputs including
756 the pronounced decline from the peak in the 1980s until the much lower recent values were prescribed (Meier et
757 al., 2018a). Hence, in ECOSUPPORT the nutrient input reductions under the BSAP between future and
758 historical inputs are smaller than in BalticAPP/CLIMSEA resulting in a smaller response of the biogeochemical
759 cycling. We argue that the more realistic historical simulation including a spinup since 1850 under observed or
760 reconstructed nutrient inputs as used for the BalticAPP and CLIMSEA ensembles would give a more realistic
761 model response compared to the ECOSUPPORT scenario simulations. However, not exactly known current and



762 completely unknown future bioavailable nutrient inputs from land and atmosphere were classified as one of the
763 biggest uncertainties (Meier et al., 2019b).

764

765 The various ensembles of scenario simulations have in common that plausible nutrient input changes have a
766 bigger impact on changes in biogeochemical variables such as nutrients, phytoplankton and oxygen
767 concentrations than projected changes in climate such as warming or changes in vertical stratification. The latter
768 would be caused by freshwater increase, SLR or changes in regional wind fields assuming RCP4.5 or RCP8.5
769 scenarios. Long-term simulations of past climate supported these results. Although historical warming had an
770 impact on the size of present-day hypoxic area, model results suggested that the main reason for hypoxia in the
771 Baltic Sea were the increase in nutrient inputs due to population growth and intensified agriculture since 1950
772 (Gustafsson et al., 2012; Carstensen et al., 2014; Meier et al., 2012a; 2019c, d). Hypoxia was also observed
773 during the medieval climate anomaly (Zillén and Conley, 2010). However, paleoclimate modeling could not
774 explain such conditions without substantial increases in nutrient inputs (Schimanke et al., 2012). Thus, the
775 sensitivity of state-of-the-art physical-biogeochemical to various drivers might be questioned and models do not
776 reproduce all important processes correctly.

777

778 For a more detailed discussion of uncertainties in Baltic Sea projections, the reader is referred to Meier et al.
779 (2018a; 2019b; 2021).

780 **5 Summary**

781 The latest published scenario simulations confirm the findings of the first and second assessments of climate
782 change in the Baltic Sea region (BACC Author Team, 2008; BACC II Author Team, 2015), namely that in all
783 projections driven by RCP4.5 and RCP8.5 and driven by four selected ESMs of CMIP5, water temperature is
784 projected to increase and sea-ice cover to decrease significantly. In the two GHG concentration scenarios,
785 ensemble mean annual SST changes between 1978-2007 and 2069-2098 amount to 2 and 3°C, respectively.
786 Warming would enhance the stability across the seasonal thermocline and mixed layer depth during summer
787 would be shallower. During winter, however, the mixed layer in the northern Baltic Sea would be deeper
788 probably because of the declining sea ice cover and the associated intensification of wind speed, waves and
789 vertical mixing. Both frequency and duration of marine heat waves would increase significantly, in particular
790 south of 60°N and in particular in the coastal zone (except in regions with frequent upwelling).

791

792 Projected spatial patterns of seasonal SST trends during 2006-2099 are similar compared to those in historical
793 reconstructions during 1850-2008 although in most regions the magnitude of trends are larger. Largest trends
794 were found in summer in the northern Baltic Sea (Bothnian Sea and Bothnian Bay) in regions where on average
795 under a warmer climate sea ice would melt earlier or would even have disappeared completely. With increasing
796 warming, SST trends in the northern Baltic Sea would get larger relative to SST trends in the southern Baltic Sea
797 indicating a weaker north-south SST gradient in future. The latter might be caused by the ice-albedo feedback.

798

799 Contrary to previous scenario simulations, recent scenario simulations considered the impact of global mean
800 SLR on Baltic Sea salinity causing a more or less complete compensation for the projected increasing river



801 runoff. However, as future changes in all three drivers of salinity, i.e. wind, runoff and SLR, are very uncertain,
802 the spread in salinity projections solely caused by the various ESMs is larger than any signal.

803

804 In agreement with the earlier assessments, we conclude that SLR has a greater potential to increase surge levels
805 in the Baltic Sea than does increased wind speed or changed wind direction.

806

807 In agreement with earlier studies, nutrient inputs changes of the BSAP or REF scenarios would have a larger
808 impact on biogeochemical cycling in the Baltic Sea than changing climate driven by RCP4.5 or RCP8.5
809 scenarios. Further, the impact of climate change would be more pronounced under higher than under lower
810 nutrient conditions. However, the response in recent studies differ from the results of previous studies
811 considerably because of more plausible assumptions on historical and future nutrient inputs resulting, for
812 instance, in sometimes opposite signs in the response of bottom oxygen concentrations. The new scenarios
813 suggest that the implementation of the BSAP would lead to a significant improvement in the ecological status of
814 the Baltic Sea regardless of the applied RCP scenario.

815

816 However, as a new driver global SLR was identified. Depending on the combination of SLR and RCP scenario, a
817 significant impact on bottom oxygen concentration was found. Higher mean sea level relative to the seabed at
818 the sills would cause increased saltwater inflows, stronger vertical stratification in the Baltic Sea and larger
819 hypoxic area. The relationship between vertical stratification and hypoxic area was confirmed by historical
820 measurements. Nevertheless, recent studies suggested that the difference in future nutrient emissions between the
821 BSAP and REF scenarios is a more important driver of changes in hypoxic area, phytoplankton concentration,
822 water transparency (expressed by Secchi depth), primary production and nitrogen fixation than projected
823 changes in climate.

824

825 The available ensembles of scenario simulations are now larger than in previous studies. It was shown that the
826 uncertainty caused by ESM differences became now also larger. However, the ensemble size might still be too
827 small and the model uncertainty is very likely underestimated. Further, natural variability might be a more
828 important source of uncertainty than previously estimated.

829

830 In present climate, the climate variability of the Baltic Sea region during winter is dominated by the impact of
831 the NAO. However, during past climate the correlation between NAO and regional variables such as water
832 temperature or sea ice varied in time. These low-frequency changes in correlation were projected to continue and
833 systematic changes in the influence of the large-scale atmospheric circulation on regional climate and in the
834 NAO itself could not be detected, although a northward shift in the mean summer position of the westerlies at
835 the end of the twenty-first century compared to the twentieth century was reported earlier (Gröger et al., 2019).

836 **Acknowledgements**

837 This study belongs to the series of Baltic Earth Assessment Reports (BEARs) of the Baltic Earth program (Earth
838 System Science for the Baltic Sea Region). The work was financed by the Copernicus Marine Environment
839 Monitoring Service through the CLIMSEA project (Regionally downscaled climate projections for the Baltic and

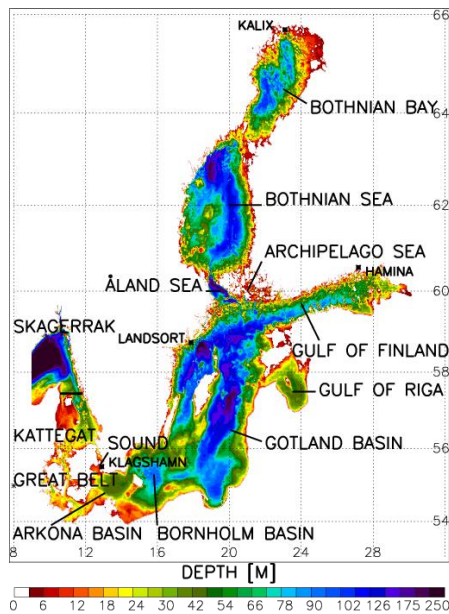


840 North seas, CMEMS 66-SE-CALL2: LOT4) and by the Swedish Research Council for Environment,
841 Agricultural Sciences and Spatial Planning (Formas) through the ClimeMarine project within the framework of
842 the National Research Programme for Climate (grant no 2017-01949). Regional climate scenario simulations
843 have been conducted on the Linux clusters Krypton, Bi, Triolith and Tetralith, all operated by the National
844 Supercomputer Centre in Sweden (NSC, <http://www.nsc.liu.se/>). Resources on Triolith and Tetralith were
845 funded by the Swedish National Infrastructure for Computing (SNIC) (grants SNIC 002/12-25, SNIC 2018/3-
846 280 and SNIC 2019/3-356). Further, we thank Berit Recklebe (Leibniz Institute for Baltic Sea Research
847 Warnemünde, IOW) for technical support.
848



849

850 **Figures**



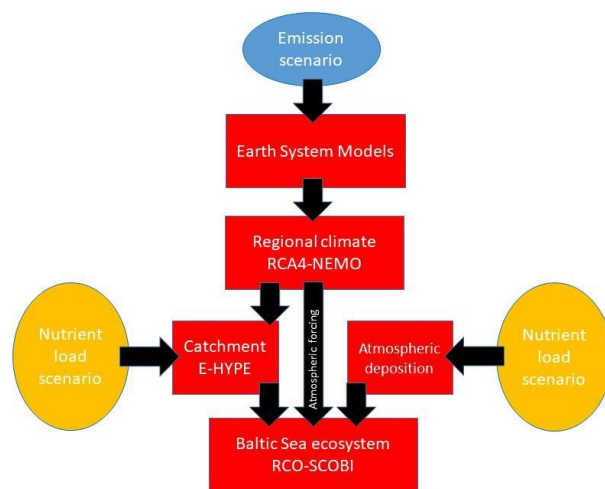
851

852 **Figure 1:** Bottom topography of the Baltic Sea (depth in m). The Baltic proper comprises the Arkona Basin,
853 Bornholm Basin and Gotland Basin. The border of the analyzed domain of the Baltic Sea models is shown as
854 black line in the northern Kattegat. In addition, the tide gauges Klagshamn (55.522°N, 12.894°E), Landsort
855 (58.742°N, 17.865°E), Hamina (60.563°N, 27.179°E), and Kalix (65.697°N, 23.096°E) are shown.

856



857



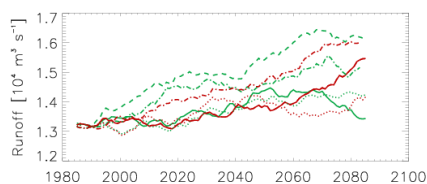
858

859 **Figure 2.** Dynamical downscaling approach for the Baltic Sea region. In Section 2, the models for the various
860 components of the Earth System are explained. (Source: Meier et al., 2021)

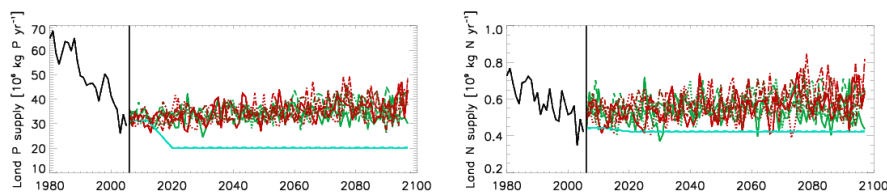
861



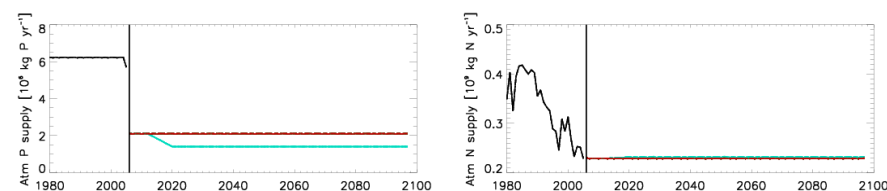
862



863



864



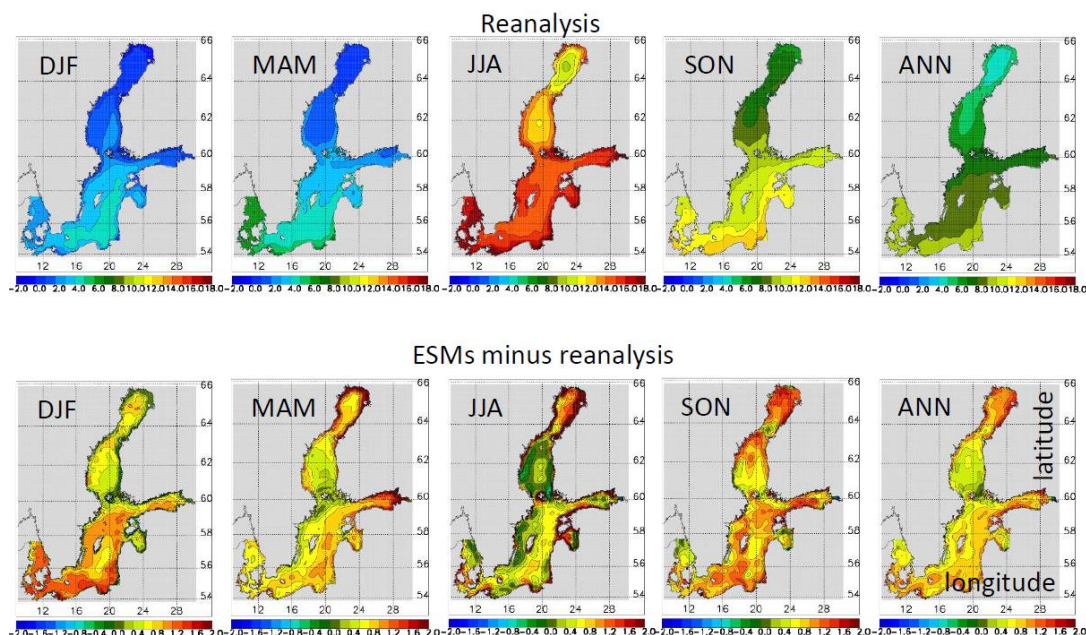
865

866 **Figure 3.** Projections of river discharge and nutrient inputs from land and atmosphere into the entire Baltic Sea
867 in BalticAPP and CLIMSEA scenario simulations. Upper panel: Low-pass filtered runoff data (in $m^3 s^{-1}$) using a
868 cut-off period of 30 years of four regionalized ESMs (illustrated by different line types) under RCP4.5 (green)
869 and RCP8.5 (red) scenarios. Lower panels: Bioavailable phosphorus (in $10^6 kg P yr^{-1}$, left panels) and nitrogen
870 inputs (in $10^9 kg N yr^{-1}$, right panels) from land (upper panels) and atmosphere (lower panels) under RCP4.5,
871 BSAP (blue), RCP4.5, REF (green), RCP8.5, BSAP (orange) and RCP8.5, REF (red) scenarios. Nutrient inputs
872 during the historical period are depicted in black. The nutrient input scenario WORST of the BalticAPP scenario
873 simulations (Saraiva et al., 2019a; their Fig. 4) and the ECOSUPPORT nutrient input scenarios (Gustafsson et
874 al., 2011; their Fig. 3.1) are not displayed here. (Source: Meier et al., 2021)

875



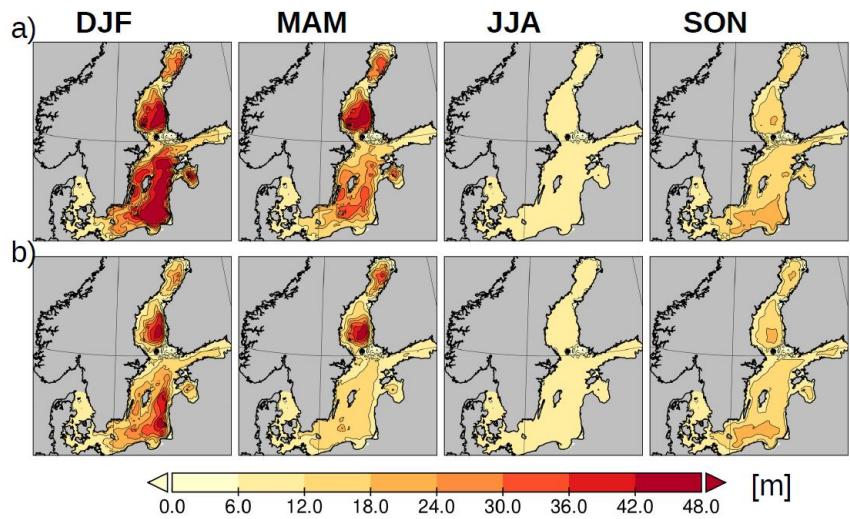
876



877

878 **Figure 4:** Upper panels: Annual and seasonal mean sea surface temperature (SST) (in °C) in reanalysis data
879 during 1970-1999 (Liu et al., 2017). Lower panels: Difference between climatologies of the ensemble mean of
880 the regionalized ESMs used in BalticAPP (Saraiva et al., 2019a) and CLIMSEA (Meier et al., 2021) during the
881 historical period (1976-2005) and of the reanalysis data. From the left to the right panels: winter (December–
882 February, DJF), spring (March–May, MAM), summer (June–August, JJA), autumn (September–November,
883 SON) and annual (ANN) mean SSTs or SST differences are shown.

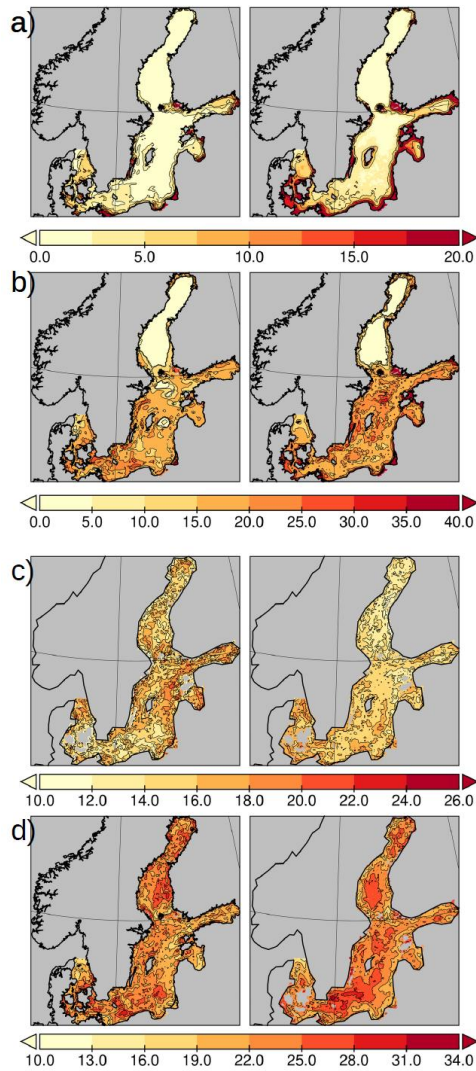
884



885

886 **Figure 5:** Mixed layer thickness calculated according to the 0.03 kg m^{-3} criterion following (de Boyer Montégut
887 et al., 2004). a) Reanalysis data (Liu et al., 2017). b) Ensemble mean over the four models (Saraiva et al., 2019a).
888 Shown are averages over 1976-1999.

889



890

891 **Figure 6:** a) Number of >10-day periods where SST is > 20°C. b) Average duration of periods displayed in a). c)

892 Number of 10-day periods where the SST is >95th percentile. d) Average duration periods displayed in c). Left

893 column: reanalysis data (Liu et al., 2017). Right column: ensemble mean of the scenario simulations driven by

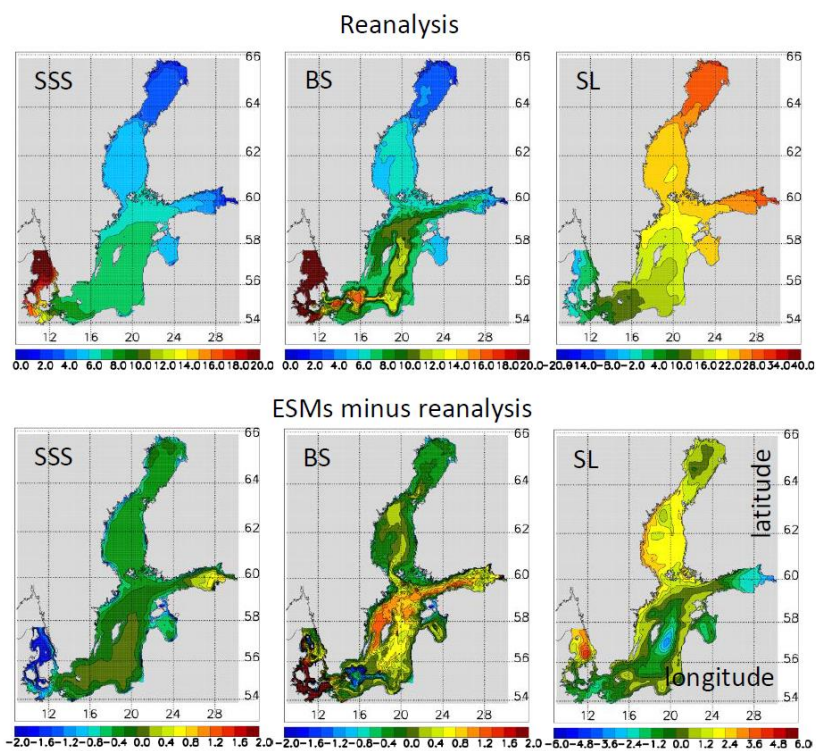
894 four ESMs (Saraiva et al., 2019a). The analysis period is 1976-1999. Note the different color scales used in c)

895 and d).

896



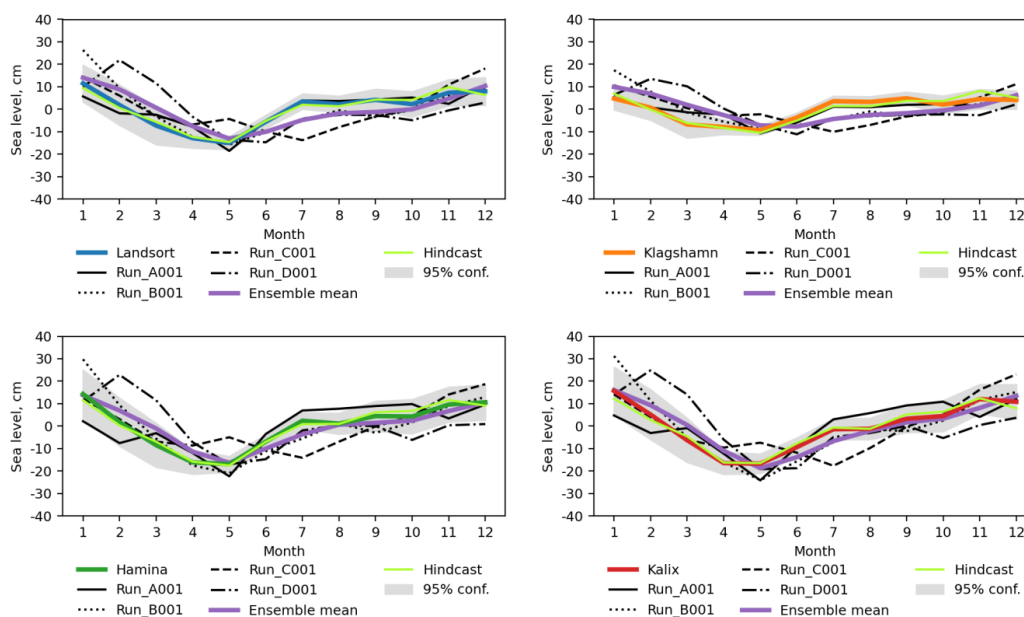
897



898

899 **Figure 7:** Upper panels: Annual mean sea surface salinity (SSS) and bottom salinity (BS) (in g kg⁻¹) and winter
900 (December–February) mean sea level (SL) (in cm) in reanalysis data during 1971-1999 (Liu et al., 2017) (from
901 left to right). Note that the model results of the sea level are given in the Nordic height system 1960 (NH60) by
902 Ekman and Mäkinen (1996). Lower panels: Difference between climatologies of the ensemble mean of the
903 regionalized ESMs used in BalticAPP (Saraiva et al., 2019a) during the historical period (1976-2005) and of the
904 reanalysis data.

905



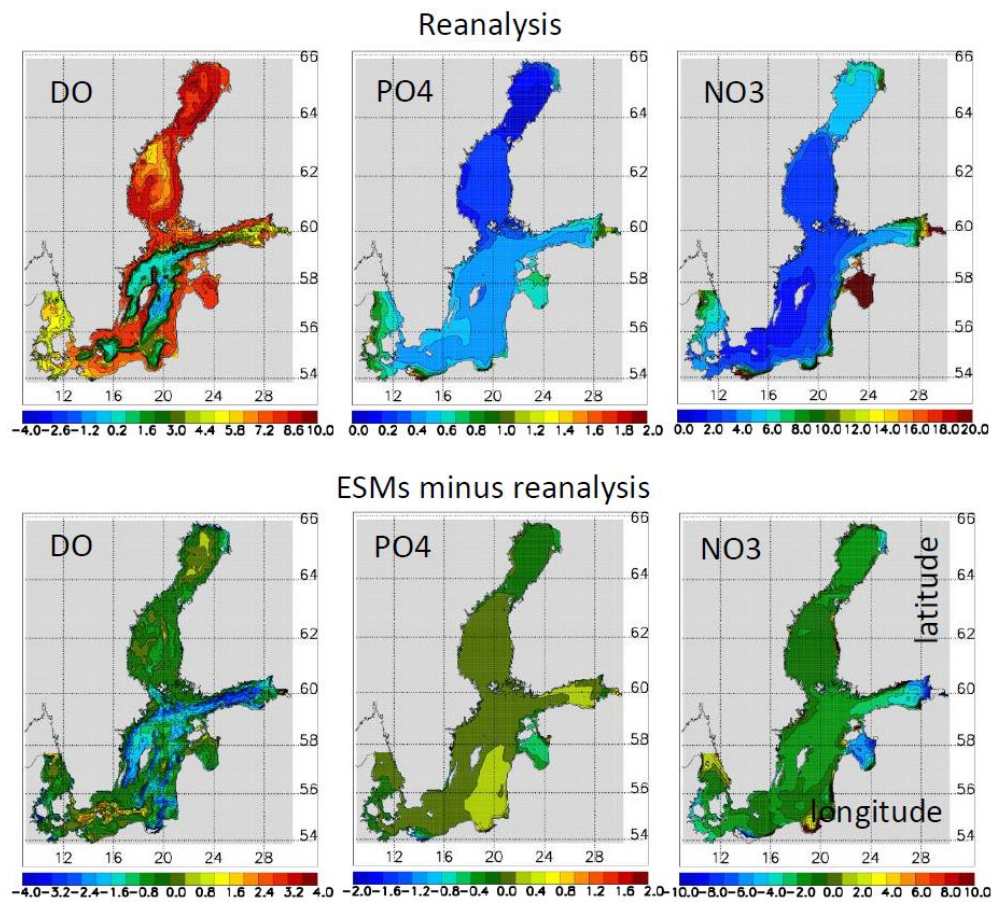
906

907 **Figure 8:** Monthly mean sea level of one hindcast (driven by regionalized reanalysis atmospheric surface fields)
908 and four climate simulations (Saraiva et al., 2019a), the ensemble mean and observations for the historical period
909 1976-2005 at the sea level stations Klagshamn, Landsort, Hamina and Kalix (for the locations see Figure 1).

910



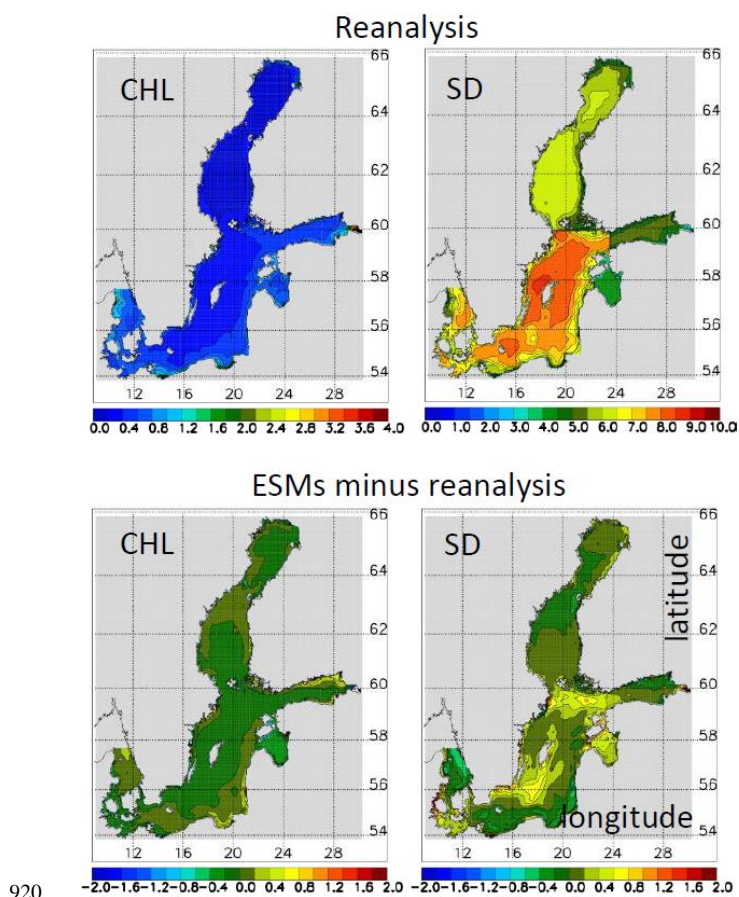
911



912

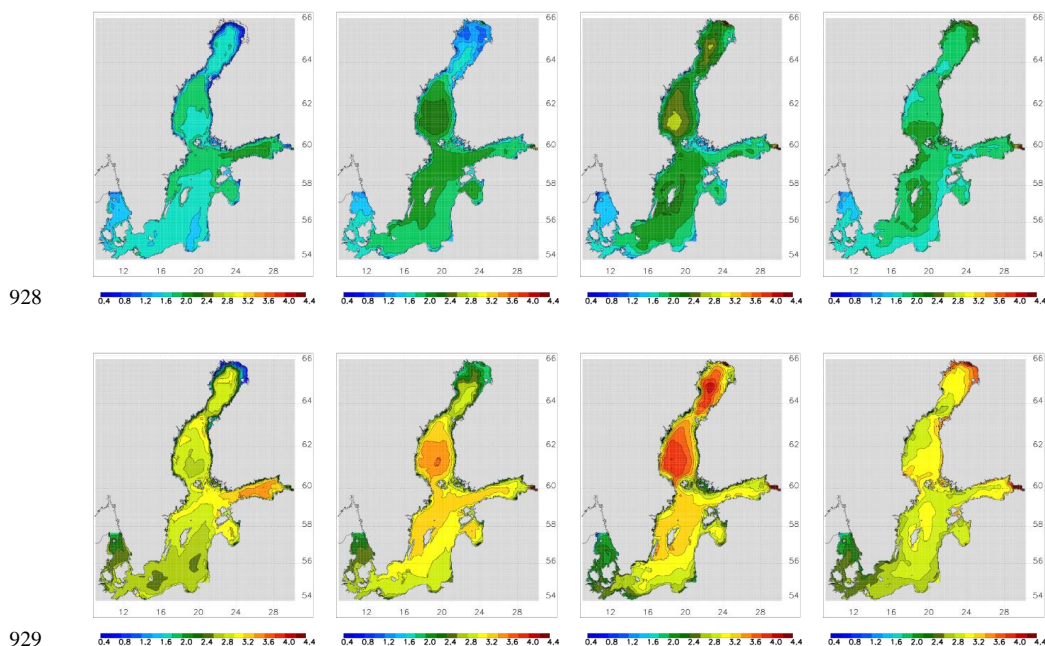
913 **Figure 9:** Upper panels: Summer (June–August) mean bottom dissolved oxygen (DO) concentrations (in mL L⁻¹), winter (December–February) mean surface phosphate (PO4) concentrations (in mmol P m⁻³) and winter (December–February) mean surface nitrate (NO3) concentrations (in mmol N m⁻³) in reanalysis data during 1976-1999 (Liu et al., 2017). Nutrient concentrations are vertically averaged for the upper 10 m. Lower panels: Difference between climatologies of the ensemble mean of the ESMs (Saraiva et al., 2019a) and the reanalysis data during the historical period (1976-2005).

919

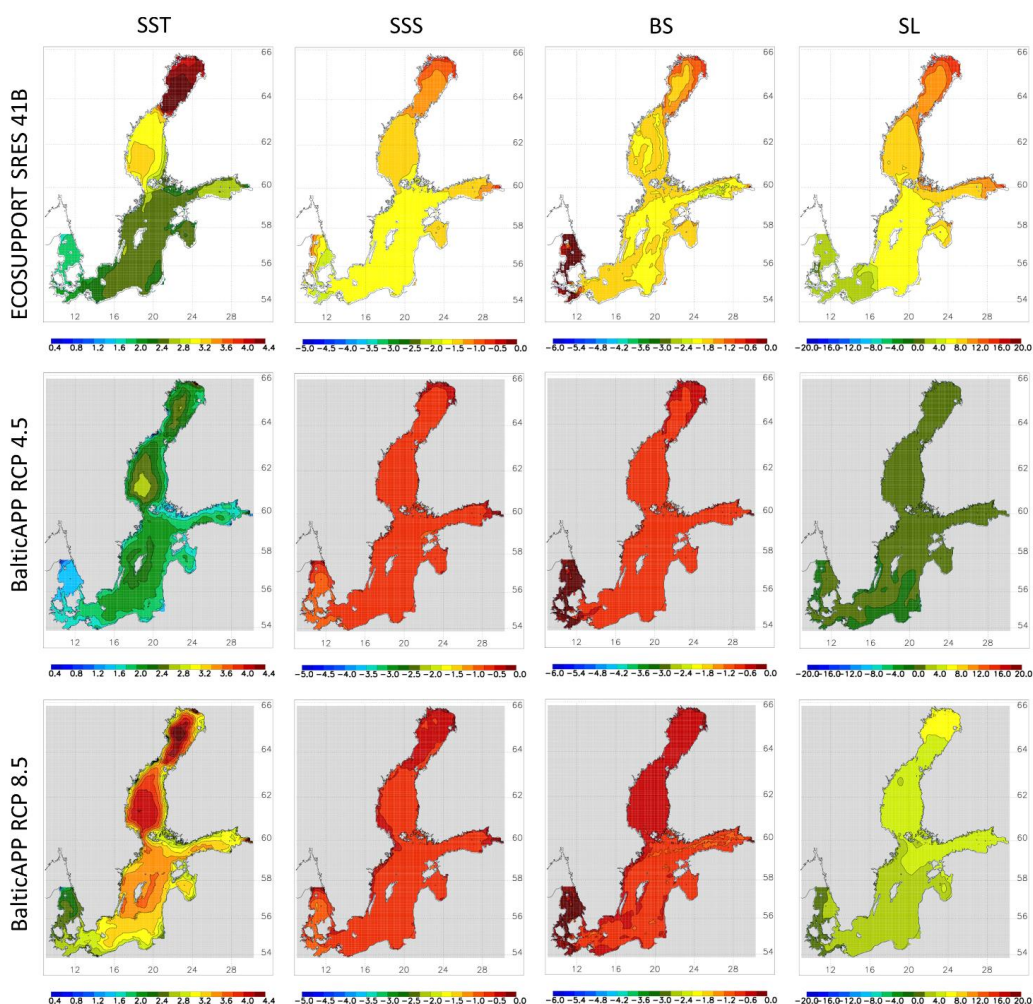


921 **Figure 10:** Upper panels: Annual mean phytoplankton concentrations (CHL) (in mg Chl m⁻³) and annual mean
922 Secchi depth (SD) (in cm) in reanalysis data during 1976-1999 (Liu et al., 2017). Phytoplankton concentrations
923 are vertically averaged for the upper 10 m. As for the calculation of Secchi depth as background only one value
924 for the concentration of yellow substances per sub-basin is available, artificial borders between sub-basins
925 become visible. Lower panels: Difference between climatologies of the ensemble mean of the ESMs (Saraiva et
926 al., 2019a) and the reanalysis data during the historical period (1976-2005).

927



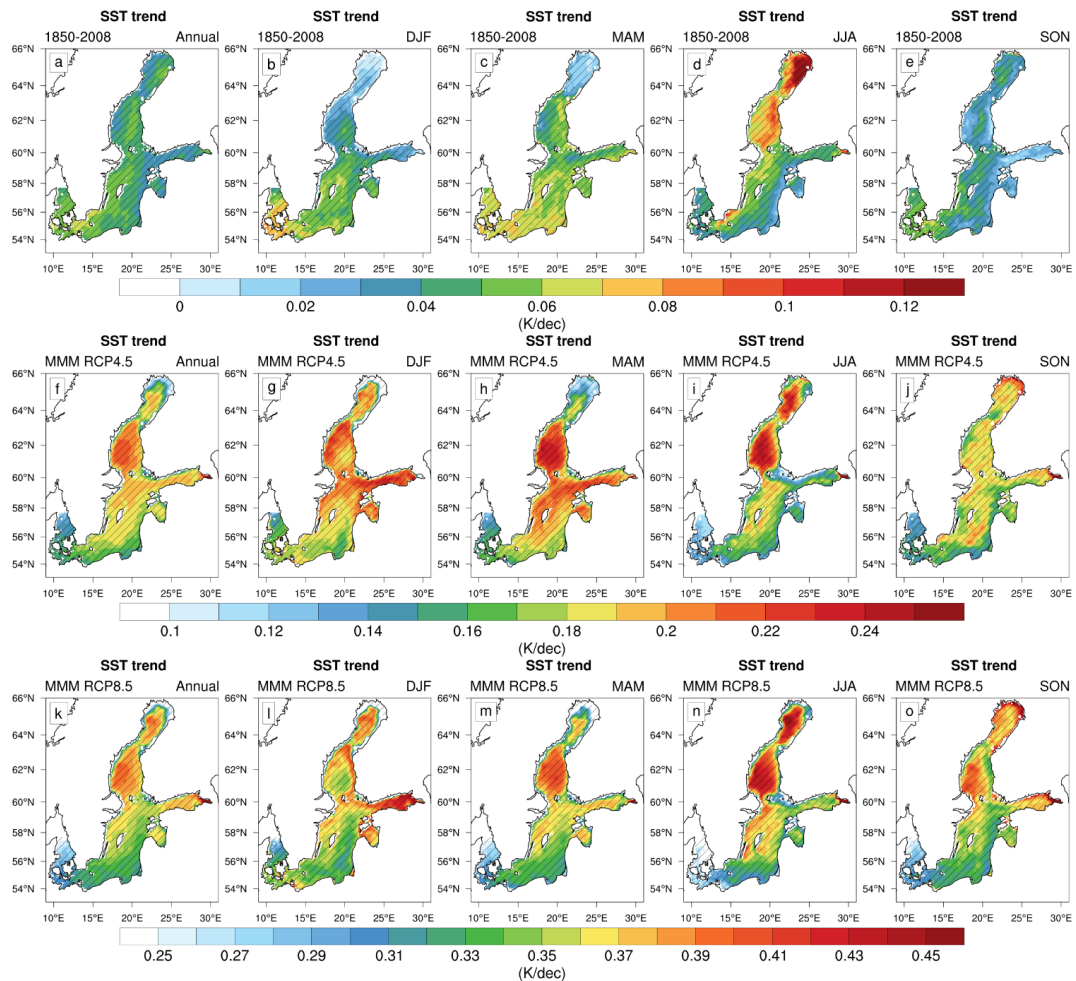
930 **Figure 11.** Changes in seasonal mean sea surface temperatures simulated by the CLIMSEA ensemble (Meier et
931 al., 2021). From left to right, winter (December, January and February; DJF), spring (March, April and May;
932 MAM), summer (June, July and August; JJA) and autumn (September, October and November; SON) mean sea
933 surface temperature changes (in °C) between 1976-2005 and 2069-2098 under RCP4.5 (upper panels) and
934 RCP8.5 (lower panels) are shown.
935



936

937 **Figure 12:** From left to right changes of summer (June – August) mean sea surface temperature (SST) (°C),
938 annual mean sea surface salinity (SSS) (g kg⁻¹), annual mean bottom salinity (BS) (g kg⁻¹), and winter
939 (December – February) mean sea level (SL) (cm) between 1978-2007 and 2069-2098 are shown. From top to
940 bottom results of the ensembles ECOSUPPORT (white background, Meier et al., 2011a), BalticAPP RCP4.5
941 (grey background, Saraiva et al., 2019a) and BalticAPP RCP8.5 (grey background, Saraiva et al., 2019a) are
942 depicted.

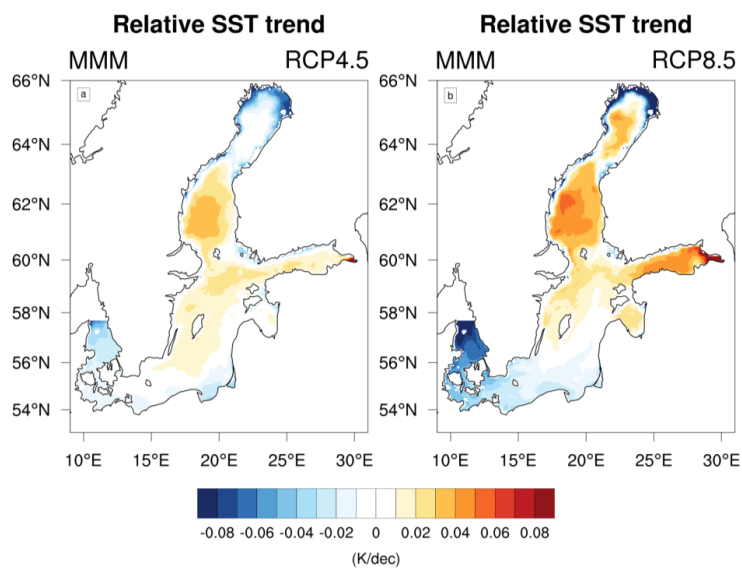
943



944

945 **Figure 13:** Multi-model mean (MMM) of annual (panels a and f) and seasonal (panels b-e and g-j) SST trends
 946 (in K decade⁻¹) computed for the period 1850-2008 (top), 2006-2099 in RCP4.5 (middle) and RCP8.5 (bottom)
 947 scenario. Hatched areas represent the regions where the trend is statistically significant (p-value<0.05, Mann-
 948 Kendall test). Data sources for historical reconstructions and projections are Meier et al. (2019d) and Saraiva et
 949 al. (2019a), respectively.

950



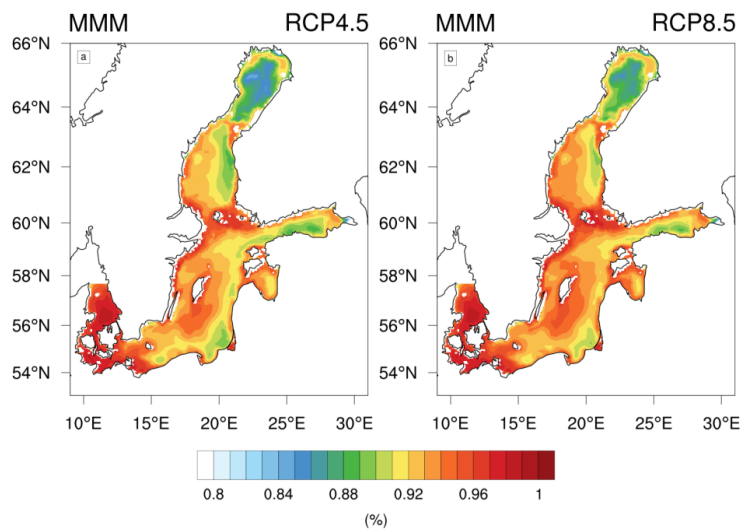
951

952 **Figure 14:** Multi-model mean of annual SST trends relative to spatial average (in K decade⁻¹) for a) RCP4.5 and
953 b) RCP8.5 scenario simulations. (Data source: Saraiva et al., 2019a)

954



955



956

957

958

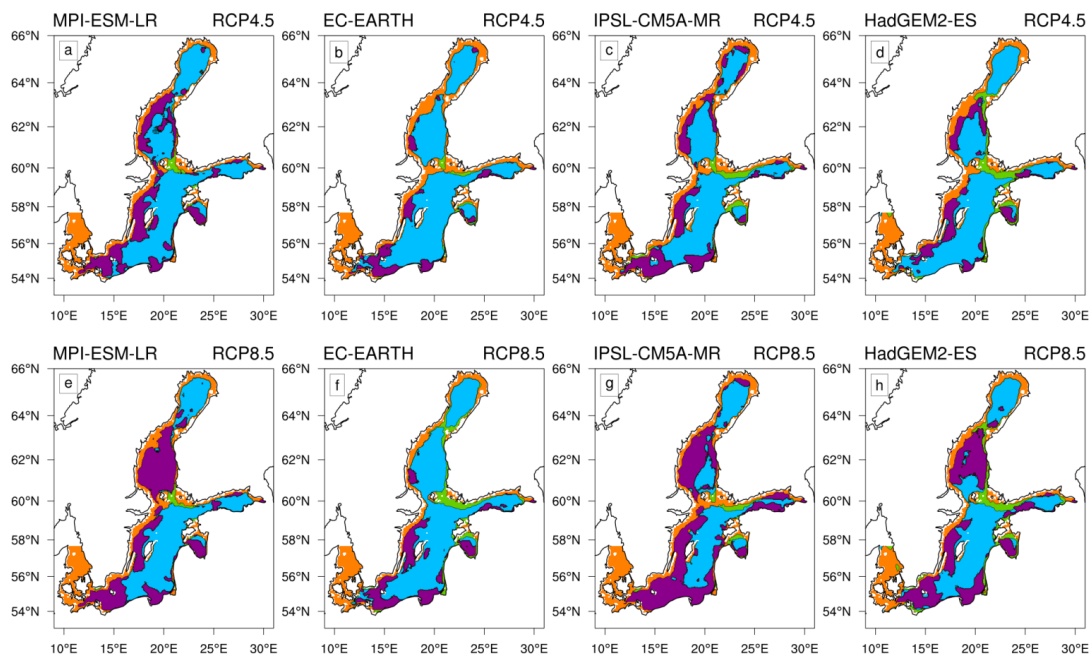
959

960

Figure 15: Multi-model mean explained variance (in percent) between the monthly mean sea surface temperature and the forcing air temperature over 2006-2099 period in a) RCP4.5 and b) RCP8.5 scenario. (Data source: Saraiva et al., 2019a)



961

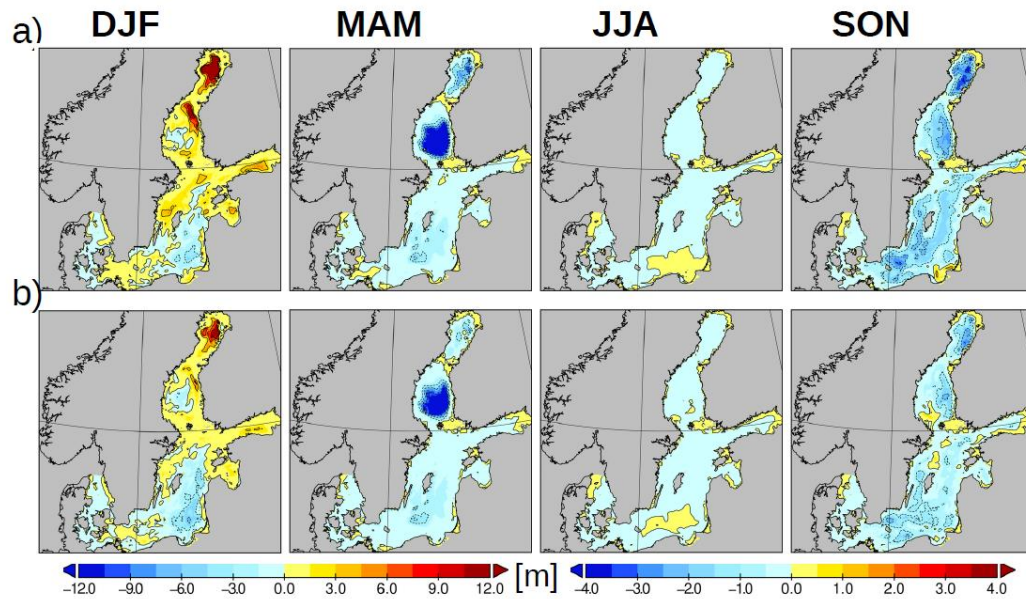


962

963

Figure 16: Results of the cross-correlation analysis of the detrended sea surface temperature (monthly mean is used) with the wind components, latent heat flux, and cloudiness. Maps of atmospheric drivers with the highest cross correlations in RCP4.5 (top) and RCP8.5 (bottom) scenarios for various GCMs forcings (Saraiva et al., 2019a). From left to right: MPI-ESM-LR, EC-EARTH, IPSL-CMA-MR, HadGEM2-ES.

967



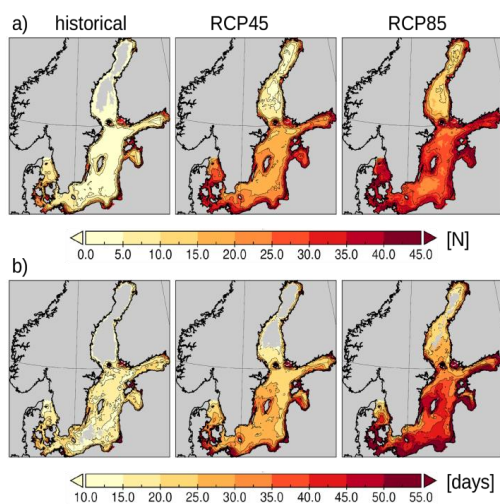
968
969

970 **Figure 17.** Mixed layer depth calculated after the 0.03 kg m^{-3} criterion after de Boyer Montégut et al. (2004).
971 Shown are ensemble average changes of four different ESMs between 1976-2005 and 2069-2098 with the mean
972 sea level rises (a) 0.90 m (RCP8.5) and (b) 0.54 m (RCP4.5). (Data source: Meier et al., 2021)

973



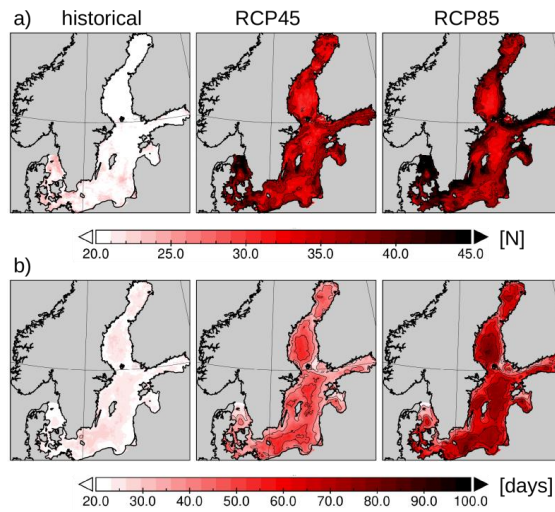
974



975

976 **Figure 18.** a) Heat waves (defined as periods of ≥ 10 days with a water temperature of $\geq 20^\circ\text{C}$) for historical
977 (1976-2005), and future (2069-2098) climates. b) Average duration of heat waves Note that no temperature bias
978 adjustment was done prior to the analysis. Shown are ensemble averages of four different ESMs with the mean
979 sea level rises (a) 0.54 m (RCP4.5) and (b) 0.90 m (RCP8.5). (Data source: Meier et al., 2021)

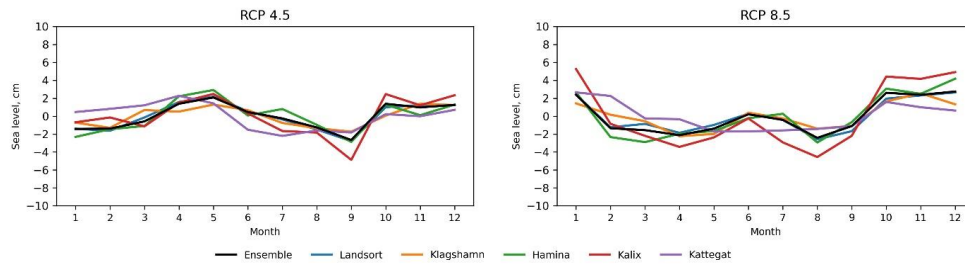
980



981

982 **Figure 19.** As Fig. 18 but for heat waves defined as periods of ≥ 10 days with a water temperature of ≥ 95 th
983 percentile of the historical reference temperature. (Data source: Meier et al., 2021)

984



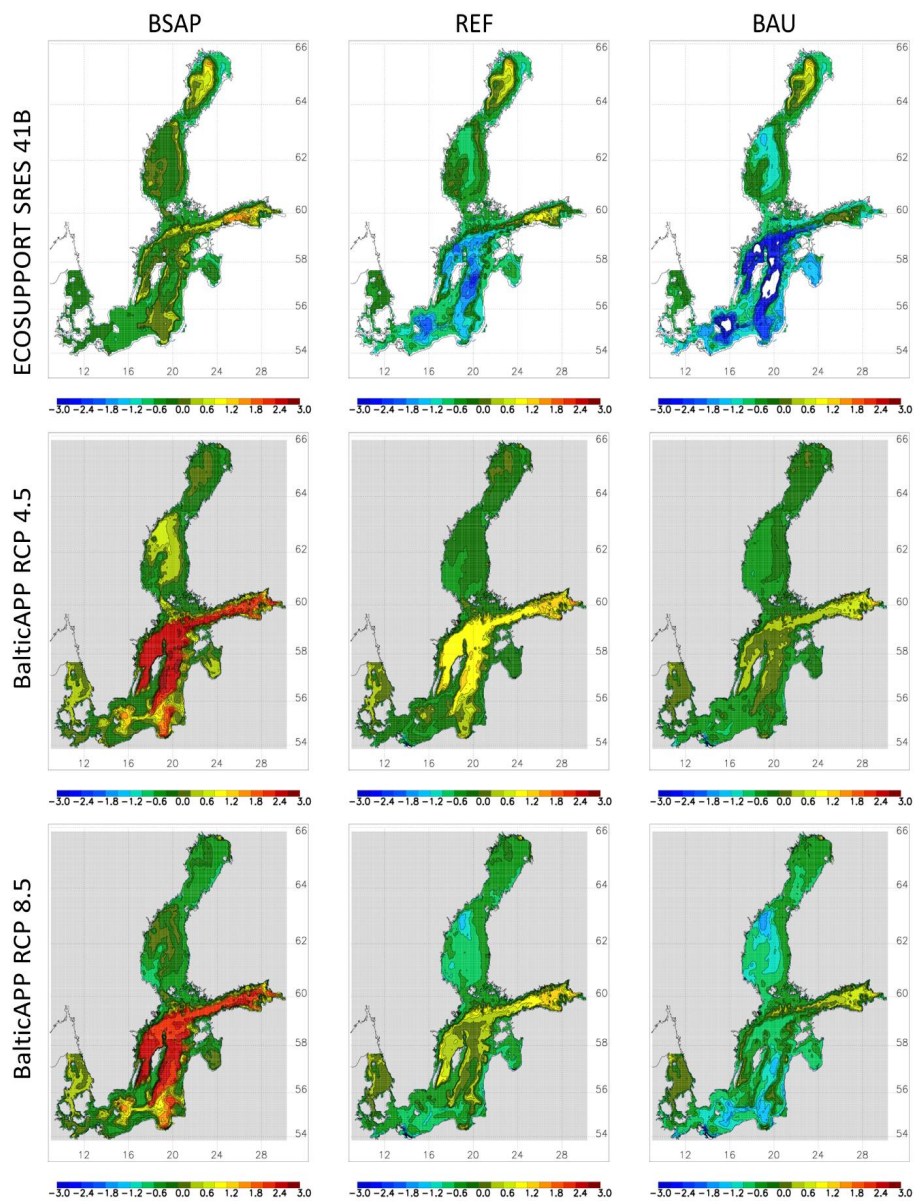
985

986 **Figure 20:** Monthly mean sea level changes between 1976-2005 and 2069-2098 at Klagshamn, Landsort,
987 Hamina, Kalix and Kattegat (for the locations see Figure 1) for RCP4.5 (left panel) and RCP8.5 (right panel).
988 Shown are the changes relative to the mean sea level rise (a) 0.54 m (RCP4.5) and (b) 0.90 m (RCP8.5). The
989 chosen model approach does not indicate any non-linear effects for larger sea level rise scenarios. (Data source:
990 Meier et al., 2021)

991



992 (a)



993

994

995

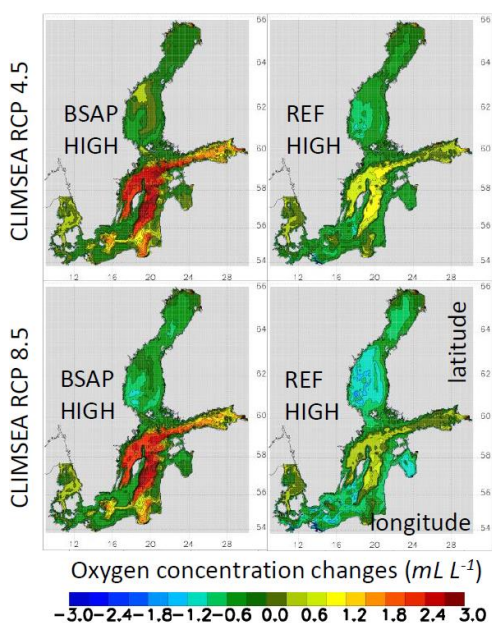
996

997

998



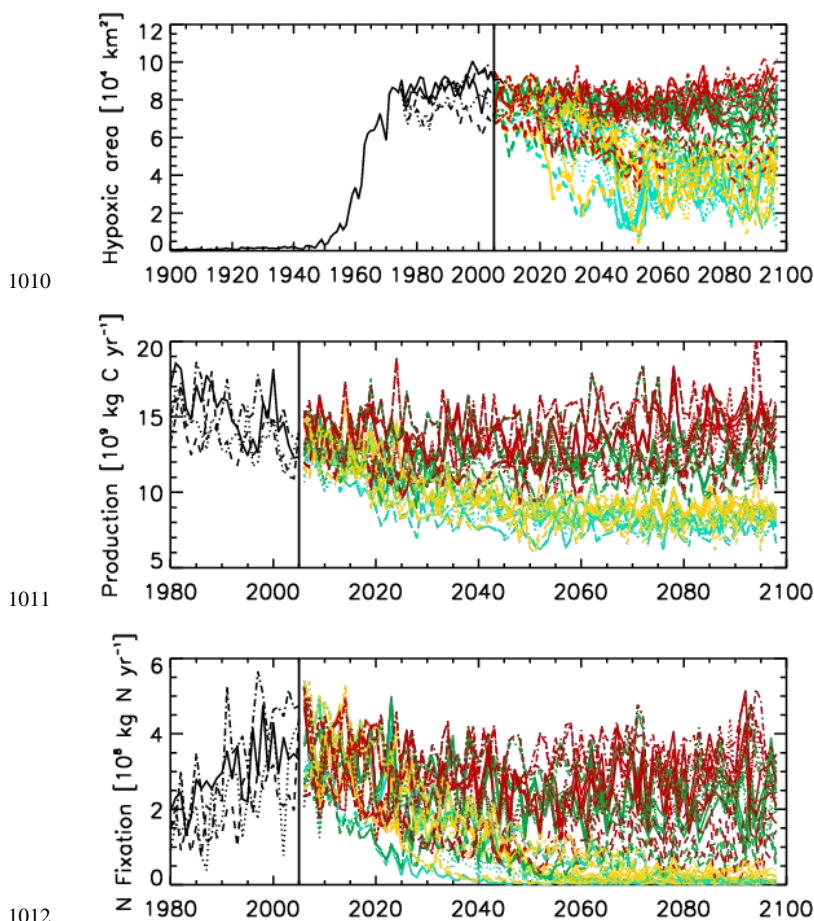
999 (b)



1000

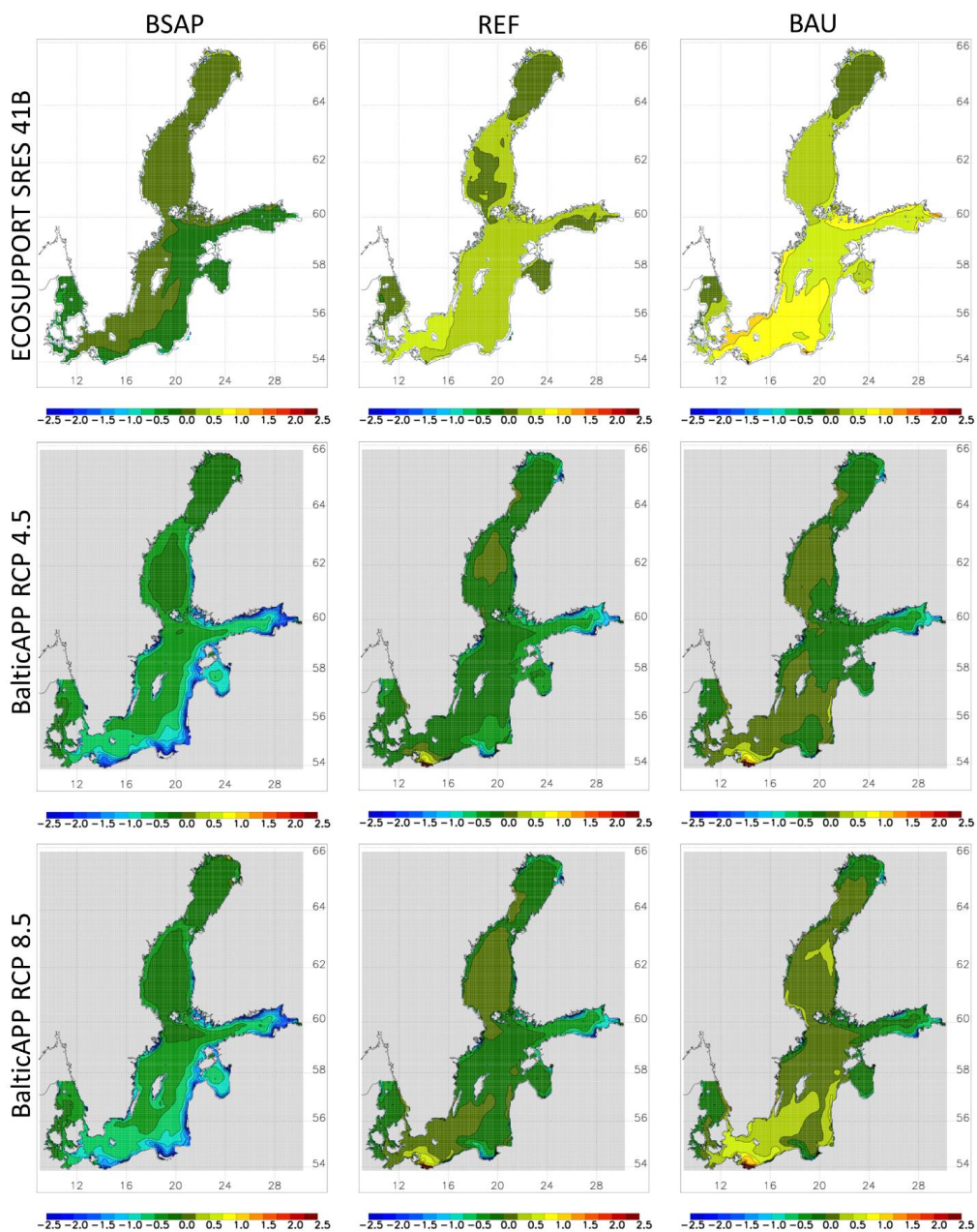
1001 **Figure 21:** (a) Ensemble mean summer (June – August) bottom dissolved oxygen concentration changes (mL L^{-1})
 1002 ¹⁾ between 1978–2007 and 2069–2098. From left to right results of the nutrient input scenarios Baltic Sea Action
 1003 Plan (BSAP), Reference (REF) and Business-As-Usual (BAU) are shown. From top to bottom results of the
 1004 ensembles ECOSUPPORT (white background, (Meier et al., 2011a)), BalticAPP RCP4.5 (grey background,
 1005 (Saraiva et al., 2019a)) and BalticAPP RCP8.5 (grey background, (Saraiva et al., 2019a)) are depicted. (b) As
 1006 panel (a) but for CLIMSEA RCP4.5 (upper panels) and CLIMSEA RCP8.5 (lower panels) under the high SLR
 1007 scenario, i.e. 1.26 m (RCP4.5) and 2.34 m (RCP8.5). Left and right columns show BSAP and REF scenarios,
 1008 respectively. (Source: Meier et al., 2021)

1009



1013 **Figure 22:** From top to bottom: hypoxic area (in km^2), volume-averaged primary production (in kg C yr^{-1}) and
1014 volume-averaged nitrogen fixation (in kg N yr^{-1}) for the entire Baltic Sea, including the Kattegat (see Fig. 1) in
1015 historical (≤ 2005 , black lines) and scenario simulations (> 2005 , coloured lines) driven by four regionalised
1016 ESMs (illustrated by different line types) under RCP4.5, BSAP (blue), RCP4.5, REF (green), RCP8.5, BSAP
1017 (orange) and RCP8.5, REF (red) scenarios. A spin-up simulation since 1850 was performed as illustrated by the
1018 evolution of hypoxia. (Source: Meier et al., 2021)

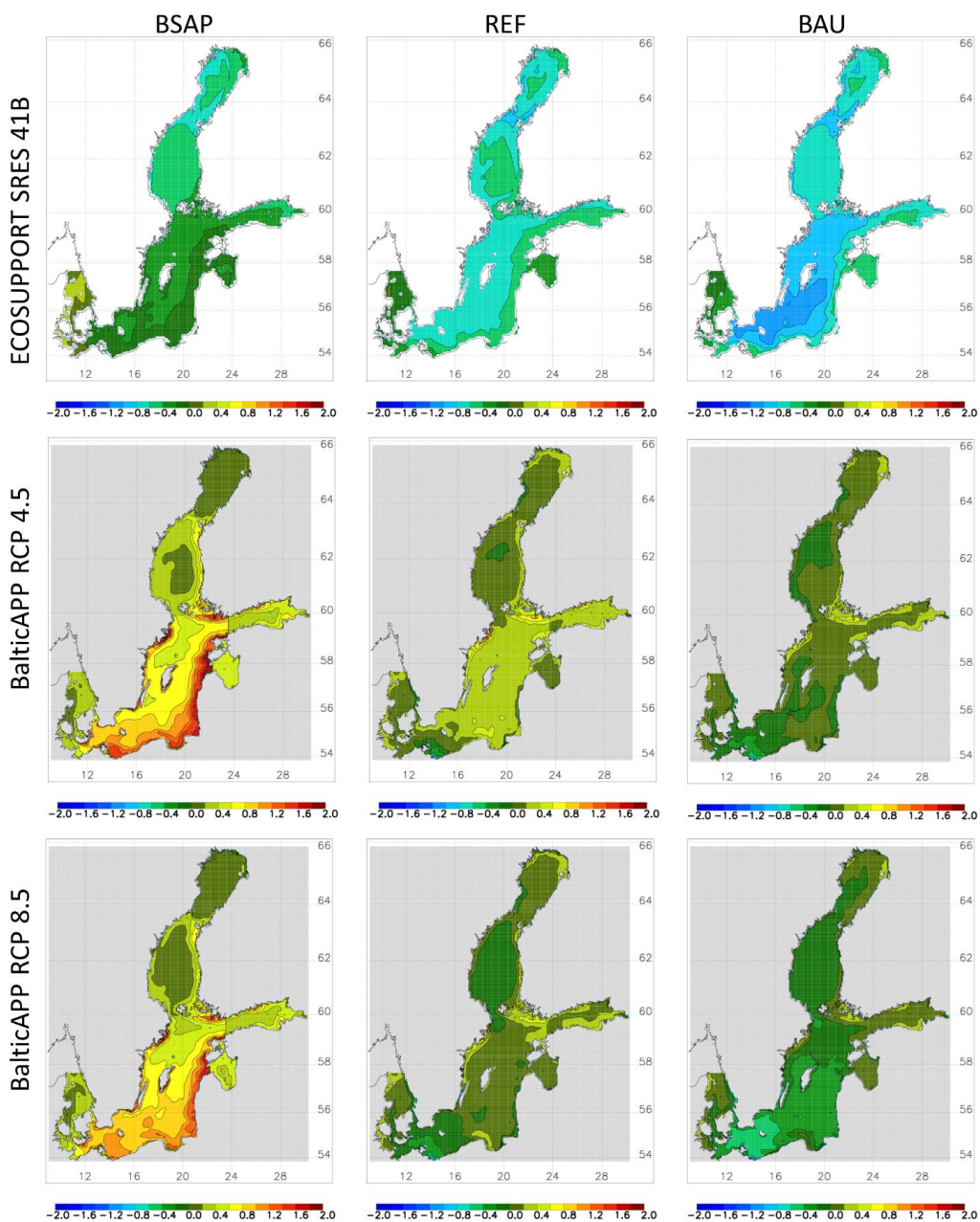
1019



1020

1021 **Figure 23:** As Fig. 21a but for annual mean surface phytoplankton concentration changes (mg Chl m⁻³).
1022 Concentrations are vertically averaged for the upper 10 m. (Source: Meier et al., 2011a; Saraiva et al., 2019a)

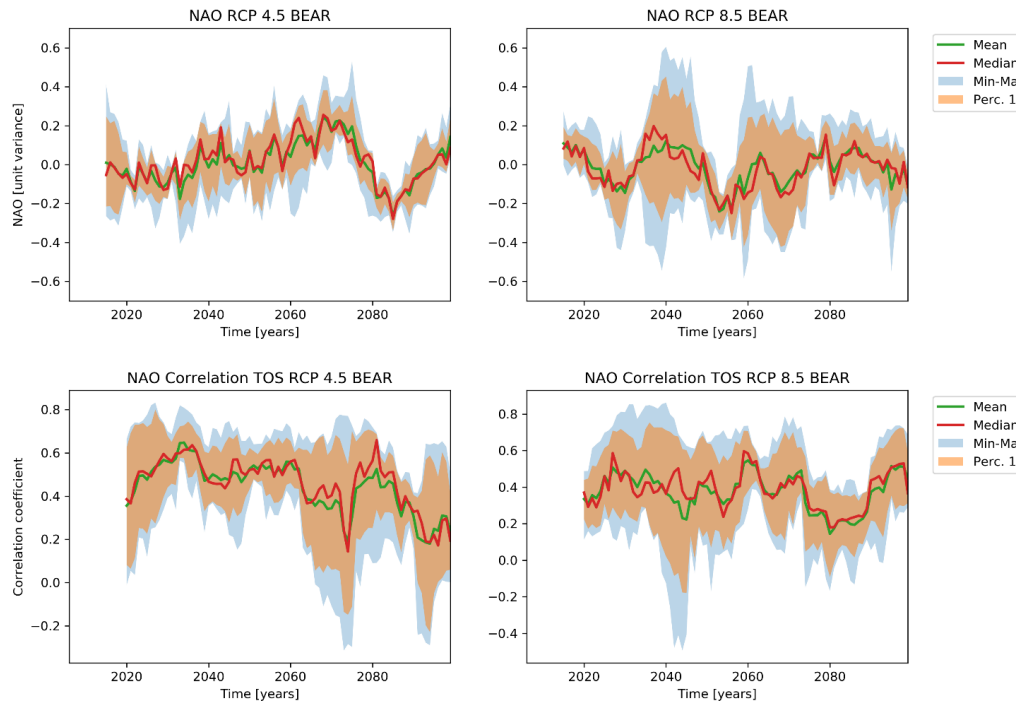
1023



1024

1025 **Figure 24.** As Fig. 21a but for annual mean Secchi depth changes (m). (Source: Meier et al., 2011a; Saraiva et
1026 al., 2019a)

1027



1028

1029

1030 **Figure 25.** Ensemble mean North Atlantic Oscillation (NAO) index (upper panels) and 10-year running
1031 correlation between NAO and area averaged sea surface temperature (SST) in the Baltic Sea (lower panels)
1032 under RCP4.5 (left panels) and RCP8.5 (right panels) scenarios. (Data source: Meier et al., 2021)

1033



1034 **Tables**

1035 **Table 1.** Selected ensembles of scenario simulations for the Baltic Sea carried out in international projects (AR =
 1036 IPCC Assessment Report, GCM = General Circulation Model, RCSM = Regional Climate System Model,
 1037 RCAO = Rossby Centre Atmosphere Ocean model, RCA4 = Rossby Centre Atmosphere model Version 4,
 1038 NEMO = Nucleus for European Modelling of the Ocean, REMO = Regional Model, MPIOM = Max Planck
 1039 Institute Ocean Model, HAMSOM = Hamburg Shelf Ocean Model)

Project	Swedish Regional Climate Modeling Program	Advanced modeling tool for scenarios of the Baltic Sea ECOSystem to SUPPORT decision making	Holocene saline water inflow changes into the Baltic Sea, ecosystem responses and future scenarios	Building predictive capability regarding the Baltic Sea organic/inorganic carbon and oxygen systems	Wellbeing from the Baltic Sea - applications combining natural science and economics	Impacts of Climate Change on Waterways and Navigation	Regionally downscaled climate projections for the Baltic and North Seas
Acronym	SWECLIM	ECOSUPPORT	INFLOW	Baltic-C	BalticAPP	KLIWAS	CLIMSEA
Duration	1997-2003	2009-2011	2009-2011	2009-2011	2015-2017	2009-2013	2018-2020
Project summaries	Rummukainen et al., 2004	Meier et al., 2014	Kotilainen et al., 2014	Omstedt et al., 2014	Saraiva et al., 2019a	Bülow et al., 2014	Dieterich et al., 2019
GCMs	AR3	AR4	AR4	AR4	AR5	AR4/AR5	AR5
RCSM	RCAO	RCAO	RCAO	RCA	RCA4-NEMO	REMO-MPIOM, REMO-HAMSOM, RCA4-NEMO	RCA4-NEMO
Horizontal resolution atmosphere/ocean	50 km/10.8 km	25 km/3.6 km	25 km/3.6 km and 50 km/3.6 km for paleoclimate	25 km /horizontally integrated	25 km /3.6 km	varying	25 km/3.6 km
Period(s)	1961–1990 and 2071–2100	1961-2099	1961-2099 and 950-1800 AD	1960-2100	1976-2100, improved initial conditions	1961-2099	1976-2100
Ocean model	One physical Baltic Sea model	Three physical-biogeochemical Baltic Sea models	See ECOSUPPORT	One physical-biogeochemical Baltic Sea model including the carbon cycle	One physical-biogeochemical Baltic Sea model	Two physical regional models with focus on the Baltic Sea and North Sea regions and one physical-biogeochemical ocean model	One physical-biogeochemical Baltic Sea model
References	Döscher and Meier, 2004; Meier et al., 2004a; Meier et al., 2004b	Meier et al., 2011a; Meier et al., 2012c; Neumann et al., 2012	See ECOSUPPORT, Schimanke and Meier, 2016	Omstedt et al., 2012	Saraiva et al., 2019a, b; Meier et al., 2019b	Bülow et al., 2014; Gröger et al., 2019; Dieterich et al., 2019	Gröger et al., 2021b; Meier et al., 2021

1040



1041 **Table 2.** Salinity projections assessed by BACC Author Team (2008), BACC II Author Team (2015) and BEAR
1042 (this study). Salinity changes depend on changes in the wind field (in particular in the west wind component),
1043 river discharge and sea level rise (SLR).

	West wind	River discharge	Sea level rise	Salinity
BACC (2008)	Large increase	-8 to +26%	0	0 to -3.7 g kg ⁻¹
BACC II (2015)	Small increase	+15 to +22%	0	-1 to -2 g kg ⁻¹
BEAR (this study)	No significant change	+2 to +22%	Medium SLR +0.54 to +0.90 m	No robust change with a considerable spread

1044

1045



1046 **Table 3.** List of scenario simulations of three ensembles. From left to right, the columns show the Earth System
 1047 Model (ESM), the Regional Climate System Model (RCSM), the Baltic Sea ecosystem model, the greenhouse
 1048 gas emission or concentration scenario, the nutrient input scenario, the sea level rise (SLR) scenario and the
 1049 simulation period including historical and scenario periods. For the three SLR scenarios in the CLIMSEA
 1050 ensemble, the mean sea level changes at the end of the century are given in meters.

ECOSUPPORT (28 scenario simulations, Meier et al., 2011a)						
HadCM3	RCAO	BALTSEM	A1B	BSAP/REF/BAU	0	1961-2099
ECHAM5/MPI-OM-r1	RCAO	BALTSEM	A1B	BSAP/REF/BAU	0	1961-2099
ECHAM5/MPI-OM-r3	RCAO	BALTSEM	A1B	BSAP/REF/BAU	0	1961-2099
ECHAM5/MPI-OM-r1	RCAO	BALTSEM	A2	BSAP/REF/BAU	0	1961-2099
HadCM3	RCAO	ERGOM	A1B	BSAP/REF	0	1961-2099
ECHAM5/MPI-OM-r1	RCAO	ERGOM	A1B	BSAP/REF	0	1961-2099
HadCM3	RCAO	RCO-SCOBI	A1B	BSAP/REF/BAU	0	1961-2099
ECHAM5/MPI-OM-r1	RCAO	RCO-SCOBI	A1B	BSAP/REF/BAU	0	1961-2099
ECHAM5/MPI-OM-r3	RCAO	RCO-SCOBI	A1B	BSAP/REF/BAU	0	1961-2099
ECHAM5/MPI-OM-r1	RCAO	RCO-SCOBI	A2	BSAP/REF/BAU	0	1961-2099
BalticAPP (21 scenario simulations, Saraiva et al., 2019a)						
MPI-ESM-LR	RCA4-NEMO	RCO-SCOBI	RCP4.5	BSAP/REF/WORST	0	1976-2099
MPI-ESM-LR	RCA4-NEMO	RCO-SCOBI	RCP8.5	BSAP/REF/WORST	0	1976-2099
EC-EARTH	RCA4-NEMO	RCO-SCOBI	RCP4.5	BSAP/REF/WORST	0	1976-2099
EC-EARTH	RCA4-NEMO	RCO-SCOBI	RCP8.5	BSAP/REF/WORST	0	1976-2099
IPSL-CM5A-MR	RCA4-NEMO	RCO-SCOBI	RCP4.5	BSAP/REF/WORST	0	1976-2099
HadGEM2-ES	RCA4-NEMO	RCO-SCOBI	RCP4.5	BSAP/REF/WORST	0	1976-2098
HadGEM2-ES	RCA4-NEMO	RCO-SCOBI	RCP8.5	BSAP/REF/WORST	0	1976-2098
CLIMSEA (48 scenario simulations, Meier et al., 2021)						
MPI-ESM-LR	RCA4-NEMO	RCO-SCOBI	RCP4.5	BSAP/REF	0/0.54/1.26	1976-2099
MPI-ESM-LR	RCA4-NEMO	RCO-SCOBI	RCP8.5	BSAP/REF	0/0.90/2.34	1976-2099
EC-EARTH	RCA4-NEMO	RCO-SCOBI	RCP4.5	BSAP/REF	0/0.54/1.26	1976-2099
EC-EARTH	RCA4-NEMO	RCO-SCOBI	RCP8.5	BSAP/REF	0/0.90/2.34	1976-2099
IPSL-CM5A-MR	RCA4-NEMO	RCO-SCOBI	RCP4.5	BSAP/REF	0/0.54/1.26	1976-2099



IPSL-CM5A-MR	RCA4-NEMO	RCO-SCOBI	RCP8.5	BSAP/REF	0/0.90/2.34	1976-2099
HadGEM2-ES	RCA4-NEMO	RCO-SCOBI	RCP4.5	BSAP/REF	0/0.54/1.26	1976-2098
HadGEM2-ES	RCA4-NEMO	RCO-SCOBI	RCP8.5	BSAP/REF	0/0.90/2.34	1976-2098

1051

1052



1053 **Table 4.** Ensemble mean changes in sea surface temperature (SST) (in °C) in ECOSUPPORT, BalticAPP
1054 RCP4.5, BalticAPP RCP8.5, CLIMSEA RCP4.5 and CLIMSEA RCP8.5 scenario simulations averaged for the
1055 Baltic Sea including the Kattegat (Data sources: Meier et al., 2011a; 2021; Saraiva et al., 2019a). (DJF =
1056 December, January, February, MAM = March, April, May, JJA = June, July, August, SON = September,
1057 October, November)

Δ SST	DJF	MAM	JJA	SON	Annual mean
ECOSPPORT SRES A1B	2.5	2.8	2.8	2.5	2.6
BalticAPP RCP4.5	1.7	1.9	2.0	1.8	1.8
BalticAPP RCP8.5	2.9	3.2	3.3	3.0	3.1
CLIMSEA RCP4.5	1.7	1.9	2.0	1.9	1.9
CLIMSEA RCP8.5	2.8	3.0	3.0	2.9	2.9

1058

1059



1060 **Table 5.** Ensemble mean changes in annual mean sea surface salinity (SSS) (in g kg⁻¹), annual mean bottom
 1061 salinity (BS) (in g kg⁻¹) and winter mean sea level (SL) relative to the global mean sea level (in cm) in
 1062 ECOSUPPORT, BalticAPP RCP4.5, BalticAPP RCP8.5, CLIMSEA RCP4.5 and CLIMSEA RCP8.5 scenario
 1063 simulations averaged for the Baltic Sea including the Kattegat. For CLIMSEA, both the ensemble mean and the
 1064 high sea level scenarios are listed. In ECOSUPPORT and BalticAPP/CLIMSEA changes between 1978-2007
 1065 and 2069-2098 and between 1976-2005 and 2069-2098 were calculated, respectively. (Data sources: Meier et al.,
 1066 2011a; 2021; Saraiva et al., 2019a)

Annual/winter changes	ECOSUPPORT A1B/A2	BalticAPP RCP4.5	BalticAPP RCP8.5	CLIMSEA RCP4.5 mean	CLIMSEA RCP4.5 high	CLIMSEA RCP8.5 mean	CLIMSEA RCP8.5 high
Δ SSS	-1.5	-0.7	-0.6	-0.3	+0.2	-0.2	+0.6
Δ BS	-1.6	-0.6	-0.6	-0.0	+0.6	-0.0	+1.1
Δ SL	+5.5	+0.4	+3.7	+0.2	+0.1	+3.4	+3.2

1067

1068



1069 **Table 6.** As Table 5, but ensemble mean changes in summer mean bottom oxygen concentration (in mL L⁻¹) in
 1070 ECOSUPPORT, BalticAPP RCP4.5, BalticAPP RCP8.5, CLIMSEA RCP4.5 and CLIMSEA RCP8.5 scenario
 1071 simulations averaged for the Baltic Sea including the Kattegat. The project changes depend on the nutrient input
 1072 scenario Baltic Sea Action Plan (BSAP), Reference (REF) and Business-As-Usual (BAU) or Worst Case
 1073 (WORST). (Data sources: Meier et al., 2011a; 2021; Saraiva et al., 2019a)

Summer changes	ECOSUPPORT A1B/A2	BalticAPP RCP4.5	BalticAPP RCP8.5	CLIMSEA RCP4.5 mean	CLIMSEA RCP4.5 high	CLIMSEA RCP8.5 mean	CLIMSEA RCP8.5 high
BSAP	-0.1	+0.6	+0.5	+0.6	+0.5	+0.4	+0.3
REF	-0.6	+0.1	-0.2	+0.0	-0.1	-0.2	-0.4
BAU/WORST	-1.1	-0.1	-0.5	-	-	-	-

1074

1075



1076 **Table 7.** As Table 5, but ensemble mean changes in annual Secchi depth (in m) in ECOSUPPORT, BalticAPP
 1077 RCP4.5, BalticAPP RCP8.5, CLIMSEA RCP4.5 and CLIMSEA RCP8.5 scenario simulations averaged for the
 1078 Baltic Sea including the Kattegat. The project changes depend on the nutrient input scenario Baltic Sea Action
 1079 Plan (BSAP), Reference (REF) and Business-As-Usual (BAU) or Worst Case (WORST). (Data sources: Meier
 1080 et al., 2011a; 2021; Saraiva et al., 2019a)

Annual changes	ECOSUPPORT A1B/A2	BalticAPP RCP4.5	BalticAPP RCP8.5	CLIMSEA RCP4.5 mean	CLIMSEA RCP4.5 high	CLIMSEA RCP8.5 mean	CLIMSEA RCP8.5 high
BSAP	-0.1	+0.6	+0.5	+0.6	+0.6	+0.6	+0.6
REF	-0.6	+0.1	-0.2	+0.2	+0.2	+0.1	+0.1
BAU/WORST	-1.1	-0.1	-0.5	-	-	-	-

1081

1082 **References**

1083 Almroth-Rosell, E., Eilola, K., Hordoir, R., Meier, H. E. M., and Hall, P. O. J.: Transport of fresh and
 1084 resuspended particulate organic material in the Baltic Sea - a model study, *J. Mar. Syst.*, 87, 1-12,
 1085 <https://doi.org/10.1016/j.jmarsys.2011.02.005>, 2011.

1086 Almroth-Rosell, E., Eilola, K., Kuznetsov, I., Hall, P. O. J., and Meier, H. E. M.: A new approach to model
 1087 oxygen dependent benthic phosphate fluxes in the Baltic Sea, *J. Mar. Syst.*, 144, 127-141,
 1088 <https://doi.org/10.1016/j.jmarsys.2014.11.007>, 2015.

1089 BACC Author Team: Assessment of climate change for the Baltic Sea basin, *Regional Climate Studies*, Springer
 1090 Science & Business Media, Berlin, Heidelberg, 473 pp., 2008.

1091 BACC II Author Team: Second Assessment of Climate Change for the Baltic Sea Basin, *Regional Climate
 1092 Studies*, Springer International Publishing, Cham, 2015.

1093 Bamber, J. L., Oppenheimer, M., Kopp, R. E., Aspinall, W. P., and Cooke, R. M.: Ice sheet contributions to
 1094 future sea-level rise from structured expert judgment, *P. Natl. Acad. Sci. USA*, 116, 11195,
 1095 <https://doi.org/10.1073/pnas.1817205116>, 2019.

1096 Bauer, B., Gustafsson, B. G., Hyytiäinen, K., Meier, H. E. M., Müller-Karulis, B., Saraiva, S., and Tomczak, M.
 1097 T.: Food web and fisheries in the future Baltic Sea, *Ambio*, <https://doi.org/10.1007/s13280-019-01229-3>, 2019.

1098 Belkin, I. M.: Rapid warming of large marine ecosystems, *Prog. Oceanogr.*, 81, 207-213,
 1099 <https://doi.org/10.1016/j.pocean.2009.04.011>, 2009.

1100 Beranová, R., and Huth, R.: Time variations of the effects of circulation variability modes on European
 1101 temperature and precipitation in winter, *Int. J. Climatol.*, 28, 139-158, <https://doi.org/10.1002/joc.1516>, 2008.

1102 Bergström, S., and Carlsson, B.: River runoff to the Baltic Sea - 1950-1990, *Ambio*, 23, 280-287, 1994.

1103 Börgel, F., Frauen, C., Neumann, T., Schimanke, S., and Meier, H. E. M.: Impact of the Atlantic Multidecadal
 1104 Oscillation on Baltic Sea Variability, *Geophys. Res. Lett.*, 45, 9880-9888,
 1105 <https://doi.org/10.1029/2018GL078943>, 2018.

1106 Börgel, F., Frauen, C., Neumann, T., and Meier, H. E. M.: The Atlantic Multidecadal Oscillation controls the
 1107 impact of the North Atlantic Oscillation on North European climate, *Environ. Res. Lett.*,
 1108 <https://doi.org/10.1088/1748-9326/aba925>, 2020.



- 1109 Bülow, K., Dietrich, C., Elizalde, A., Gröger, M., Heinrich, H., Hüttl-Kabos, S., Klein, B., Mayer, B., Meier, H.
1110 E. M., and Mikolajewicz, U.: Comparison of three regional coupled ocean atmosphere models for the North Sea
1111 under today's and future climate conditions (KLIWAS Schriftenreihe; KLIWAS-27/2014), Bundesanstalt für
1112 Gewässerkunde, 2014.
- 1113 Carstensen, J., Andersen, J. H., Gustafsson, B. G., and Conley, D. J.: Deoxygenation of the Baltic Sea during the
1114 last century, *P. Natl. Acad. Sci. USA*, 111, 5628-5633, <https://doi.org/10.1073/pnas.1323156111>, 2014.
- 1115 Chen, D., and Hellström, C.: The influence of the North Atlantic Oscillation on the regional temperature
1116 variability in Sweden: spatial and temporal variations, *Tellus A: Dynamic Meteorology and Oceanography*, 51,
1117 505-516, <https://doi.org/10.1034/j.1600-0870.1999.t01-4-00004.x>, 1999.
- 1118 Christensen, O. B., Kjellström, E., Dieterich, C., Gröger, M., and Meier, H. E. M.: Atmospheric regional climate
1119 projections for the Baltic Sea Region until 2100, *Earth Syst. Dynam.*, 2021.
- 1120 Church, J. A., Clark, P. U., Cazenave, A., Gregory, J. M., Jevrejeva, S., Levermann, A., Merrifield, M. A.,
1121 Milne, G. A., Nerem, R. S., Nunn, P. D., Payne, A. J., Pfeffer, W. T., Stammer, D., and Unnikrishnan, A. S.: Sea
1122 Level Change, in: *Climate Change 2013 – The Physical Science Basis: Working Group I Contribution to the*
1123 *Fifth Assessment Report of the Intergovernmental Panel on Climate Change*, edited by: Stocker, T. F., Qin, D.,
1124 Plattner, G.-K., Tignor, M., Allen, S. K., Boschung, J., Nauels, A., Xia, Y., Bex, V., and Midgley, P. M.,
1125 Cambridge University Press, Cambridge, UK, New York, USA, 1137-1216,
1126 <https://doi.org/10.1017/CBO9781107415324>, 2013.
- 1127 de Boyer Montégut, C., Madec, G., Fischer, A. S., Lazar, A., and Iudicone, D.: Mixed layer depth over the
1128 global ocean: An examination of profile data and a profile-based climatology, *J. Geophys. Res-Oceans*, 109,
1129 <https://doi.org/10.1029/2004jc002378>, 2004.
- 1130 Dieterich, C., Wang, S., Schimanke, S., Gröger, M., Klein, B., Hordoir, R., Samuelsson, P., Liu, Y., Axell, L.,
1131 and Höglund, A.: Surface heat budget over the North Sea in climate change simulations, *Atmosphere*, 10, 272,
1132 <https://doi.org/10.3390/atmos10050272>, 2019.
- 1133 Donnelly, C., Greuell, W., Andersson, J., Gerten, D., Pisacane, G., Roudier, P., and Ludwig, F.: Impacts of
1134 climate change on European hydrology at 1.5, 2 and 3 degrees mean global warming above preindustrial level,
1135 *Clim. Change*, 143, 13-26, <https://doi.org/10.1007/s10584-017-1971-7>, 2017.
- 1136 Döscher, R., Willén, U., Jones, C., Rutgersson, A., Meier, H. E. M., Hansson, U., and Graham, L. P.: The
1137 development of the regional coupled ocean-atmosphere model RCAO, *Boreal Environ. Res.*, 7, 183-192, 2002.
- 1138 Döscher, R., and Meier, H. E. M.: Simulated sea surface temperature and heat fluxes in different climates of the
1139 Baltic Sea, *Ambio*, 33, 242-248, <https://doi.org/10.1579/0044-7447-33.4.242>, 2004.
- 1140 Ehrnsten, E., Norkko, A., Müller-Karulis, B., Gustafsson, E., and Gustafsson, B. G.: The meagre future of
1141 benthic fauna in a coastal sea—Benthic responses to recovery from eutrophication in a changing climate, *Global*
1142 *Change Biol.*, 26, 2235-2250, <https://doi.org/10.1111/gcb.15014>, 2020.
- 1143 Eilola, K., Meier, H. E. M., and Almroth, E.: On the dynamics of oxygen, phosphorus and cyanobacteria in the
1144 Baltic Sea; A model study, *J. Mar. Syst.*, 75, 163-184, <https://doi.org/10.1016/j.jmarsys.2008.08.009>, 2009.
- 1145 Eilola, K., Gustafsson, B. G., Kuznetsov, I., Meier, H. E. M., Neumann, T., and Savchuk, O. P.: Evaluation of
1146 biogeochemical cycles in an ensemble of three state-of-the-art numerical models of the Baltic Sea, *J. Mar. Syst.*,
1147 88, 267-284, <https://doi.org/10.1016/j.jmarsys.2011.05.004>, 2011.
- 1148 Eilola, K., Mårtensson, S., and Meier, H. E. M.: Modeling the impact of reduced sea ice cover in future climate
1149 on the Baltic Sea biogeochemistry, *Geophys. Res. Lett.*, 40, 149-154, <https://doi.org/10.1029/2012GL054375>,
1150 2013.
- 1151 Ekman, M., and Mäkinen, J.: Mean sea surface topography in the Baltic Sea and its transition area to the North
1152 Sea: A geodetic solution and comparisons with oceanographic models, *J. Geophys. Res-Oceans*, 101, 11993-
1153 11999, <https://doi.org/10.1029/96JC00318>, 1996.



- 1154 Fleming-Lehtinen, V., and Laamanen, M.: Long-term changes in Secchi depth and the role of phytoplankton in
1155 explaining light attenuation in the Baltic Sea, *Estuar. Coast. Shelf Sci.*, 102-103, 1-10,
1156 <https://doi.org/10.1016/j.ecss.2012.02.015>, 2012.
- 1157 Fonselius, S., and Valderrama, J.: One hundred years of hydrographic measurements in the Baltic Sea, *J. Sea
1158 Res.*, 49, 229-241, [https://doi.org/10.1016/S1385-1101\(03\)00035-2](https://doi.org/10.1016/S1385-1101(03)00035-2), 2003.
- 1159 Friedland, R., Neumann, T., and Schernewski, G.: Climate change and the Baltic Sea action plan: model
1160 simulations on the future of the western Baltic Sea, *J. Mar. Syst.*, 105-108, 175-186,
1161 <https://doi.org/10.1016/j.jmarsys.2012.08.002>, 2012.
- 1162 Friedland, R., Macias, D., Cossarini, G., Daewel, U., Estournel, C., Garcia-Gorriz, E., Grizzetti, B., Grégoire,
1163 M., Gustafson, B., Kalaroni, S., Kerimoglu, O., Lazzari, P., Lenhart, H., Lessin, G., Maljutenko, I., Miladinova,
1164 S., Müller-Karulis, B., Neumann, T., Pärn, O., Pätsch, J., Piroddi, C., Raudsepp, U., Schrum, C., Stegert, C.,
1165 Stips, A., Tsiaras, K., Ulses, C., and Vandenbulcke, L.: Effects of nutrient management scenarios on marine
1166 eutrophication indicators: a Pan-European, multi-model assessment in support of the Marine Strategy
1167 Framework Directive, *Front. Mar. Sci.*, 8, 596126, <https://doi.org/10.3389/fmars.2021.596126>, 2021.
- 1168 Gogina, M., Zettler, M. L., Wählström, I., Andersson, H., Radtke, H., Kuznetsov, I., and MacKenzie, B. R.: A
1169 combination of species distribution and ocean-biogeochemical models suggests that climate change overrides
1170 eutrophication as the driver of future distributions of a key benthic crustacean in the estuarine ecosystem of the
1171 Baltic Sea, *ICES J. Mar. Sci.*, 77, 2089-2105, <https://doi.org/10.1093/icesjms/fsaa107>, 2020.
- 1172 Gräwe, U., and Burchard, H.: Storm surges in the Western Baltic Sea: the present and a possible future, *Clim.
1173 Dyn.*, 39, 165-183, <https://doi.org/10.1007/s00382-011-1185-z>, 2012.
- 1174 Gräwe, U., Friedland, R., and Burchard, H.: The future of the western Baltic Sea: two possible scenarios, *Ocean
1175 Dynam.*, 63, 901-921, <https://doi.org/10.1007/s10236-013-0634-0>, 2013.
- 1176 Grinsted, A.: Projected Change - Sea Level, in: Second Assessment of Climate Change for the Baltic Sea Basin,
1177 edited by: BACC II Author Team, *Regional Climate Studies*, Springer International Publishing, Cham, 253-263,
1178 https://doi.org/10.1007/978-3-319-16006-1_14, 2015.
- 1179 Gröger, M., Dieterich, C., Meier, H. E. M., and Schimanke, S.: Thermal air-sea coupling in hindcast simulations
1180 for the North Sea and Baltic Sea on the NW European shelf, *Tellus A: Dynamic Meteorology and
1181 Oceanography*, 67, 26911, <https://doi.org/10.3402/tellusa.v67.26911>, 2015.
- 1182 Gröger, M., Arneborg, L., Dieterich, C., Höglund, A., and Meier, H. E. M.: Summer hydrographic changes in the
1183 Baltic Sea, Kattegat and Skagerrak projected in an ensemble of climate scenarios downscaled with a coupled
1184 regional ocean-sea ice-atmosphere model, *Clim. Dyn.*, <https://doi.org/10.1007/s00382-019-04908-9>, 2019.
- 1185 Gröger, M., Dieterich, C., Ho-Hagemann, H. T. M., Hagemann, S., Jakacki, J., May, W., Meier, H. E. M.,
1186 Miller, P. A., Rutgersson, A., and Wu, L.: Coupled regional Earth system modelling in the Baltic Sea region,
1187 *Earth Syst. Dynam. Discuss.*, 1-50, <https://doi.org/10.5194/esd-2021-14>, 2021a.
- 1188 Gröger, M., Dieterich, C., and Meier, H. E. M.: Is interactive air sea coupling relevant for simulating the future
1189 climate of Europe?, *Clim. Dyn.*, 56, 491-514, <https://doi.org/10.1007/s00382-020-05489-8>, 2021b.
- 1190 Gustafsson, B. G., Savchuk, O. P., and Meier, H. E. M.: Load scenarios for ECOSUPPORT, Technical Report
1191 No. 4, Baltic Nest Institute, Stockholm, Sweden, 18, 2011.
- 1192 Gustafsson, B. G., Schenk, F., Blenkner, T., Eilola, K., Meier, H. E. M., Müller-Karulis, B., Neumann, T.,
1193 Ruoho-Airola, T., Savchuk, O. P., and Zorita, E.: Reconstructing the development of Baltic Sea eutrophication
1194 1850-2006, *Ambio*, 41, 534-548, <https://doi.org/10.1007/s13280-012-0318-x>, 2012.
- 1195 Haapala, J., Meier, H. E. M., and Rinne, J.: Numerical investigations of future ice conditions in the Baltic Sea,
1196 *Ambio*, 30, 237-244, <https://doi.org/10.1579/0044-7447-30.4.237>, 2001.
- 1197 HELCOM: Towards a Baltic Sea unaffected by eutrophication - HELCOM Overview 2007, Krakow, Poland,
1198 HELCOM Ministerial Meeting, 35, 2007.



- 1199 HELCOM: Approaches and methods for eutrophication target setting in the Baltic Sea region, Helsinki, Finland,
1200 Baltic Sea Environment Proceedings No. 133, 138pp, 2013.
- 1201 HELCOM: State of the Baltic Sea - Second HELCOM holistic assessment 2011-2016, Helsinki, Finland, Baltic
1202 Sea Environment Proceedings No. 155, 155pp, 2018.
- 1203 Hense, I., and Beckmann, A.: Towards a model of cyanobacteria life cycle—effects of growing and resting
1204 stages on bloom formation of N₂-fixing species, *Ecol. Model.*, 195, 205-218,
1205 <https://doi.org/10.1016/j.ecolmodel.2005.11.018>, 2006.
- 1206 Hense, I., and Beckmann, A.: The representation of cyanobacteria life cycle processes in aquatic ecosystem
1207 models, *Ecol. Model.*, 221, 2330-2338, <https://doi.org/10.1016/j.ecolmodel.2010.06.014>, 2010.
- 1208 Hieronymus, J., Eilola, K., Olofsson, M., Hense, I., Meier, H. E. M., and Almroth-Rosell, E.: Modeling
1209 cyanobacteria life cycle dynamics and historical nitrogen fixation in the Baltic Sea, *Biogeosciences Discuss.*,
1210 2021, 1-27, <https://doi.org/10.5194/bg-2021-156>, 2021.
- 1211 Hieronymus, M., and Kalén, O.: Sea-level rise projections for Sweden based on the new IPCC special report:
1212 The ocean and cryosphere in a changing climate, *Ambio*, <https://doi.org/10.1007/s13280-019-01313-8>, 2020.
- 1213 Hill, E. M., Davis, J. L., Tamisiea, M. E., and Lidberg, M.: Combination of geodetic observations and models for
1214 glacial isostatic adjustment fields in Fennoscandia, *J. Geophys. Res.-Sol. Ea.*, 115,
1215 <https://doi.org/10.1029/2009jb006967>, 2010.
- 1216 Hobday, A. J., Oliver, E. C. J., Gupta, A. S., Benthuyssen, J. A., Burrows, M. T., Donat, M. G., Holbrook, N. J.,
1217 Moore, P. J., Thomsen, M. S., Wernberg, T., and Smale, D. A.: Categorizing and Naming MARINE
1218 HEATWAVES, *Oceanography*, 31, 162-173, 2018.
- 1219 Höglund, A., Pemberton, P., Hordoir, R., and Schimanke, S.: Ice conditions for maritime traffic in the Baltic Sea
1220 in future climate, *Boreal Environ. Res.*, 22, 245-265, 2017.
- 1221 Holopainen, R., Lehtiniemi, M., Meier, H. E. M., Albertsson, J., Gorokhova, E., Kotta, J., and Viitasalo, M.:
1222 Impacts of changing climate on the non-indigenous invertebrates in the northern Baltic Sea by end of the twenty-
1223 first century, *Biol. Invasions*, 18, 3015-3032, <https://doi.org/10.1007/s10530-016-1197-z>, 2016.
- 1224 Holt, J., Schrum, C., Cannaby, H., Daewel, U., Allen, I., Artioli, Y., Bopp, L., Butenschon, M., Fach, B. A.,
1225 Harle, J., Pushpadas, D., Salihoglu, B., and Wakelin, S.: Potential impacts of climate change on the primary
1226 production of regional seas: A comparative analysis of five European seas, *Prog. Oceanogr.*, 140, 91-115,
1227 <https://doi.org/10.1016/j.pocean.2015.11.004>, 2016.
- 1228 Hordoir, R., and Meier, H. E. M.: Effect of climate change on the thermal stratification of the baltic sea: a
1229 sensitivity experiment, *Clim. Dyn.*, 38, 1703-1713, <https://doi.org/10.1007/s00382-011-1036-y>, 2012.
- 1230 Hordoir, R., Höglund, A., Pemberton, P., and Schimanke, S.: Sensitivity of the overturning circulation of the
1231 Baltic Sea to climate change, a numerical experiment, *Clim. Dyn.*, 50, 1425-1437,
1232 <https://doi.org/10.1007/s00382-017-3695-9>, 2018.
- 1233 Hordoir, R., Axell, L., Höglund, A., Dieterich, C., Fransner, F., Gröger, M., Liu, Y., Pemberton, P., Schimanke,
1234 S., Andersson, H., Ljungemyr, P., Nygren, P., Falahat, S., Nord, A., Jönsson, A., Lake, I., Döös, K.,
1235 Hieronymus, M., Dietze, H., Löptien, U., Kuznetsov, I., Westerlund, A., Tuomi, L., and Haapala, J.: Nemo-
1236 Nordic 1.0: a NEMO-based ocean model for the Baltic and North seas – research and operational applications,
1237 *Geosci. Model Dev.*, 12, 363-386, <https://doi.org/10.5194/gmd-12-363-2019>, 2019.
- 1238 Hundecha, Y., Arheimer, B., Donnelly, C., and Pechlivanidis, I.: A regional parameter estimation scheme for a
1239 pan-European multi-basin model, *J. Hydrol.-Reg. Stud.*, 6, 90-111, <https://doi.org/10.1016/j.ejrh.2016.04.002>,
1240 2016.
- 1241 Hünicke, B., and Zorita, E.: Influence of temperature and precipitation on decadal Baltic Sea level variations in
1242 the 20th century, *Tellus A: Dynamic Meteorology and Oceanography*, 58, 141-153,
1243 <https://doi.org/10.1111/j.1600-0870.2006.00157.x>, 2006.



- 1244 Hünicke, B., Zorita, E., Soomere, T., Madsen, K. S., Johansson, M., and Suursaar, Ü.: Recent Change—Sea
1245 Level and Wind Waves, in: Second Assessment of Climate Change for the Baltic Sea Basin, edited by: BACC II
1246 Author Team, Springer International Publishing, Cham, 155-185, 10.1007/978-3-319-16006-1_9, 2015.
- 1247 Hurrell, J. W.: Decadal trends in the North Atlantic Oscillation: regional temperatures and precipitation, Science-
1248 AAAS-Weekly Paper Edition, 269, 676-679, <https://doi.org/10.1126/science.269.5224.676> 1995.
- 1249 IPCC: Climate Change 2013 – The Physical Science Basis: Working Group I Contribution to the Fifth
1250 Assessment Report of the Intergovernmental Panel on Climate Change,
1251 <https://doi.org/10.1017/CBO9781107415324>, 2013.
- 1252 IPCC: IPCC Special Report on the Ocean and Cryosphere in a Changing Climate, edited by: Pörtner, H.-O.,
1253 Roberts, D. C., Masson-Delmotte, V., Zhai, P., Tignor, M., Poloczanska, E., Mintenbeck, K., Alegría, A.,
1254 Nicolai, M., Okem, A., Petzold, J., Rama, B., and Weyer, N. M., 2019a.
- 1255 IPCC: Summary for Policymakers, in: IPCC Special Report on the Ocean and Cryosphere in a Changing
1256 Climate, edited by: Pörtner, H.-O., Roberts, D. C., Masson-Delmotte, V., Zhai, P., Tignor, M., Poloczanska, E.,
1257 Mintenbeck, K., Alegría, A., Nicolai, M., Okem, A., Petzold, J., Rama, B., and Weyer, N. M., 2019b.
- 1258 Jacob, D., Petersen, J., Eggert, B., Alias, A., Christensen, O. B., Bouwer, L. M., Braun, A., Colette, A., Déqué,
1259 M., Georgievski, G., and others: EURO-CORDEX: new high-resolution climate change projections for European
1260 impact research, Reg. Environ. Change, 14, 563-578, <https://doi.org/10.1007/s10113-013-0499-2>, 2014.
- 1261 Jutterström, S., Andersson, H. C., Omstedt, A., and Malmaeus, J. M.: Multiple stressors threatening the future of
1262 the Baltic Sea - Kattegat marine ecosystem: Implications for policy and management actions, Mar. Pollut. Bull.,
1263 86, 468-480, <https://doi.org/10.1016/j.marpolbul.2014.06.027>, 2014.
- 1264 Kniebusch, M., Meier, H. E. M., Neumann, T., and Börgel, F.: Temperature Variability of the Baltic Sea Since
1265 1850 and Attribution to Atmospheric Forcing Variables, J. Geophys. Res-Oceans, 124, 4168-4187,
1266 <https://doi.org/10.1029/2018jc013948>, 2019.
- 1267 Kotilainen, A. T., Arppe, L., Dobosz, S., Jansen, E., Kabel, K., Karhu, J., Kotilainen, M. M., Kuijpers, A.,
1268 Loughheed, B. C., Meier, H. E. M., Moros, M., Neumann, T., Porsche, C., Poulsen, N., Rasmussen, P., Ribeiro,
1269 S., Risebrobakken, B., Ryabchuk, D., Schimanke, S., Snowball, I., Spiridonov, M., Virtasalo, J. J., Weckström,
1270 K., Witkowski, A., and Zhamoida, V.: Echoes from the Past: A Healthy Baltic Sea Requires More Effort, Ambio
1271 43, 60-68, <https://doi.org/10.1007/s13280-013-0477-4>, 2014.
- 1272 Kratzer, S., Håkansson, B., and Charlotte, S.: Assessing Secchi and Photic Zone Depth in the Baltic Sea from
1273 Satellite Data, Ambio, 32, 577-585, 2003.
- 1274 Kuznetsov, I., and Neumann, T.: Simulation of carbon dynamics in the Baltic Sea with a 3D model, J. Mar.
1275 Syst., 111-112, 167-174, <https://doi.org/10.1016/j.jmarsys.2012.10.011>, 2013.
- 1276 Lang, A., and Mikolajewicz, U.: The long-term variability of extreme sea levels in the German Bight, Ocean
1277 Sci., 15, 651-668, 2019.
- 1278 Lehmann, A., Getzlaff, K., and Harlaß, J.: Detailed assessment of climate variability in the Baltic Sea area for
1279 the period 1958 to 2009, Clim. Res., 46, 185-196, <https://doi.org/10.3354/cr00876>, 2011.
- 1280 Liu, Y., Meier, H. E. M., and Eilola, K.: Nutrient transports in the Baltic Sea – results from a 30-year physical-
1281 biogeochemical reanalysis, Biogeosciences, 14, 2113-2131, <https://doi.org/10.5194/bg-14-2113-2017>, 2017.
- 1282 MacKenzie, B. R., Meier, H. E. M., Lindegren, M., Neuenfeldt, S., Eero, M., Blenckner, T., Tomczak, M. T.,
1283 and Niiranen, S.: Impact of Climate Change on Fish Population Dynamics in the Baltic Sea: A Dynamical
1284 Downscaling Investigation, Ambio 41, 626-636, <https://doi.org/10.1007/s13280-012-0325-y>, 2012.
- 1285 Madsen, K. S., Høyer, J. L., Suursaar, Ü., She, J., and Knudsen, P.: Sea Level Trends and Variability of the
1286 Baltic Sea From 2D Statistical Reconstruction and Altimetry, Front. Earth Sci., 7,
1287 <https://doi.org/10.3389/feart.2019.00243>, 2019.



- 1288 Meier, H. E. M., Doescher, R., Coward, A. C., Nycander, J., and Döös, K.: RCO – Rossby Centre regional
1289 Ocean climate model: model description (version 1.0) and first results from the hindcast period 1992/93, SMHI,
1290 Norrköping, Sweden, 102pp, 1999.
- 1291 Meier, H. E. M.: On the parameterization of mixing in three-dimensional Baltic Sea models, *J. Geophys. Res-*
1292 *Oceans*, 106, 30997-31016, <https://doi.org/10.1029/2000JC000631>, 2001.
- 1293 Meier, H. E. M.: Regional ocean climate simulations with a 3D ice–ocean model for the Baltic Sea. Part 2:
1294 results for sea ice, *Clim. Dyn.*, 19, 255-266, <https://doi.org/10.1007/s00382-001-0225-5>, 2002a.
- 1295 Meier, H. E. M.: Regional ocean climate simulations with a 3D ice-ocean model for the Baltic Sea. Part 1: model
1296 experiments and results for temperature and salinity, *Clim. Dyn.*, 19, 237-253, [https://doi.org/10.1007/s00382-](https://doi.org/10.1007/s00382-001-0224-6)
1297 [001-0224-6](https://doi.org/10.1007/s00382-001-0224-6), 2002b.
- 1298 Meier, H. E. M., and Kauker, F.: Simulating Baltic Sea climate for the period 1902-1998 with the Rossby Centre
1299 coupled ice-ocean model, SMHI, Norrköping, Sweden, 2002.
- 1300 Meier, H. E. M., Döscher, R., and Faxén, T.: A multiprocessor coupled ice-ocean model for the Baltic Sea:
1301 Application to salt inflow, *J. Geophys. Res-Oceans*, 108, 3273, <https://doi.org/10.1029/2000JC000521>, 2003.
- 1302 Meier, H. E. M., and Kauker, F.: Modeling decadal variability of the Baltic Sea: 2. Role of freshwater inflow and
1303 large-scale atmospheric circulation for salinity, *J. Geophys. Res-Oceans*, 108,
1304 <https://doi.org/10.1029/2003JC001799>, 2003.
- 1305 Meier, H. E. M., Broman, B., and Kjellström, E.: Simulated sea level in past and future climates of the Baltic
1306 Sea, *Clim. Res.*, 27, 59-75, <https://doi.org/10.3354/cr027059>, 2004a.
- 1307 Meier, H. E. M., Döscher, R., and Halkka, A.: Simulated distributions of Baltic Sea-ice in warming climate and
1308 consequences for the winter habitat of the Baltic ringed seal, *Ambio*, 33, 249-256, [https://doi.org/10.1579/0044-](https://doi.org/10.1579/0044-7447-33.4.249)
1309 [7447-33.4.249](https://doi.org/10.1579/0044-7447-33.4.249), 2004b.
- 1310 Meier, H. E. M.: Baltic Sea climate in the late twenty-first century: a dynamical downscaling approach using two
1311 global models and two emission scenarios, *Clim. Dyn.*, 27, 39-68, <https://doi.org/10.1007/s00382-006-0124-x>,
1312 2006.
- 1313 Meier, H. E. M., Kjellström, E., and Graham, L. P.: Estimating uncertainties of projected Baltic Sea salinity in
1314 the late 21st century, *Geophys. Res. Lett.*, 33, L15705, <https://doi.org/10.1029/2006GL026488>, 2006.
- 1315 Meier, H. E. M.: Modeling the pathways and ages of inflowing salt-and freshwater in the Baltic Sea, *Estuar.*
1316 *Coast. Shelf Sci.*, 74, 610-627, <https://doi.org/10.1016/j.ecss.2007.05.019>, 2007.
- 1317 Meier, H. E. M., Andersson, H. C., Eilola, K., Gustafsson, B. G., Kuznetsov, I., Müller-Karulis, B., Neumann,
1318 T., and Savchuk, O. P.: Hypoxia in future climates: A model ensemble study for the Baltic Sea, *Geophys. Res.*
1319 *Lett.*, 38, L24608, <https://doi.org/10.1029/2011GL049929>, 2011a.
- 1320 Meier, H. E. M., Eilola, K., and Almroth, E.: Climate-related changes in marine ecosystems simulated with a 3-
1321 dimensional coupled physical-biogeochemical model of the Baltic Sea, *Clim. Res.*, 48, 31-55,
1322 <https://doi.org/10.3354/cr00968> 2011b.
- 1323 Meier, H. E. M., Höglund, A., Döscher, R., Andersson, H., Löptien, U., and Kjellström, E.: Quality assessment
1324 of atmospheric surface fields over the Baltic Sea from an ensemble of regional climate model simulations with
1325 respect to ocean dynamics, *Oceanologia*, 53, 193-227, <https://doi.org/10.5697/oc.53-1-TI.193>, 2011c.
- 1326 Meier, H. E. M., Andersson, H. C., Arheimer, B., Blenckner, T., Chubarenko, B., Donnelly, C., Eilola, K.,
1327 Gustafsson, B. G., Hansson, A., Havenhand, J., and others: Comparing reconstructed past variations and future
1328 projections of the Baltic Sea ecosystem—first results from multi-model ensemble simulations, *Environ. Res.*
1329 *Lett.*, 7, 34005, <https://doi.org/10.1088/1748-9326/7/3/034005>, 2012a.
- 1330 Meier, H. E. M., Eilola, K., Gustavsson, B. G., Kuznetsov, I., Neumann, T., and Savchuk, O. P.: Uncertainty
1331 assessment of projected ecological quality indicators in future climate, SMHI, Norrköping, Sweden, 2012b.



- 1332 Meier, H. E. M., Hordoir, R., Andersson, H. C., Dieterich, C., Eilola, K., Gustafsson, B. G., Höglund, A., and
1333 Schimanke, S.: Modeling the combined impact of changing climate and changing nutrient loads on the Baltic
1334 Sea environment in an ensemble of transient simulations for 1961–2099, *Clim. Dyn.*, 39, 2421–2441,
1335 <https://doi.org/10.1007/s00382-012-1339-7>, 2012c.
- 1336 Meier, H. E. M., Müller-Karulis, B., Andersson, H. C., Dieterich, C., Eilola, K., Gustafsson, B. G., Höglund, A.,
1337 Hordoir, R., Kuznetsov, I., Neumann, T., and others: Impact of climate change on ecological quality indicators
1338 and biogeochemical fluxes in the Baltic Sea: a multi-model ensemble study, *Ambio*, 41, 558–573,
1339 <https://doi.org/10.1007/s13280-012-0320-3>, 2012d.
- 1340 Meier, H. E. M., Andersson, H. C., Arheimer, B., Donnelly, C., Eilola, K., Gustafsson, B. G., Kotwicki, L.,
1341 Neset, T.-S., Niiranen, S., Piwowarczyk, J., Savchuk, O. P., Schenk, F., Weslawski, J. M., and Zorita, E.:
1342 Ensemble modeling of the Baltic Sea ecosystem to provide scenarios for management, *Ambio*, 43, 37–48,
1343 <https://doi.org/10.1007/s13280-013-0475-6>, 2014.
- 1344 Meier, H. E. M., Höglund, A., Eilola, K., and Almroth-Rosell, E.: Impact of accelerated future global mean sea
1345 level rise on hypoxia in the Baltic Sea, *Clim. Dyn.*, 49, 163–172, <https://doi.org/10.1007/s00382-016-3333-y>,
1346 2017.
- 1347 Meier, H. E. M., Edman, M. K., Eilola, K. J., Placke, M., Neumann, T., Andersson, H. C., Brunnabend, S.-E.,
1348 Dieterich, C., Frauen, C., Friedland, R., Gröger, M., Gustafsson, B. G., Gustafsson, E., Isaev, A., Kniebusch, M.,
1349 Kuznetsov, I., Müller-Karulis, B., Omstedt, A., Ryabchenko, V., Saraiva, S., and Savchuk, O. P.: Assessment of
1350 Eutrophication Abatement Scenarios for the Baltic Sea by Multi-Model Ensemble Simulations, *Front. Mar. Sci.*,
1351 5, <https://doi.org/10.3389/fmars.2018.00440>, 2018a.
- 1352 Meier, H. E. M., Väli, G., Naumann, M., Eilola, K., and Frauen, C.: Recently accelerated oxygen consumption
1353 rates amplify deoxygenation in the Baltic Sea, *J. Geophys. Res-Oceans*, 123, 3227–3240,
1354 <https://doi.org/10.1029/2017JC013686>, 2018b.
- 1355 Meier, H. E. M., Dieterich, C., Eilola, K., Gröger, M., Höglund, A., Radtke, H., Saraiva, S., and Wählström, I.:
1356 Future projections of record-breaking sea surface temperature and cyanobacteria bloom events in the Baltic Sea,
1357 *Ambio*, 48, 1362–1376, <https://doi.org/10.1007/s13280-019-01235-5>, 2019a.
- 1358 Meier, H. E. M., Edman, M., Eilola, K., Placke, M., Neumann, T., Andersson, H. C., Brunnabend, S.-E.,
1359 Dieterich, C., Frauen, C., Friedland, R., Gröger, M., Gustafsson, B. G., Gustafsson, E., Isaev, A., Kniebusch, M.,
1360 Kuznetsov, I., Müller-Karulis, B., Naumann, M., Omstedt, A., Ryabchenko, V., Saraiva, S., and Savchuk, O. P.:
1361 Assessment of Uncertainties in Scenario Simulations of Biogeochemical Cycles in the Baltic Sea, *Front. Mar.*
1362 *Sci.*, 6, <https://doi.org/10.3389/fmars.2019.00046>, 2019b.
- 1363 Meier, H. E. M., Eilola, K., Almroth-Rosell, E., Schimanke, S., Kniebusch, M., Höglund, A., Pemberton, P., Liu,
1364 Y., Väli, G., and Saraiva, S.: Correction to: Disentangling the impact of nutrient load and climate changes on
1365 Baltic Sea hypoxia and eutrophication since 1850, *Clim. Dyn.*, 53, 1167–1169, <https://doi.org/10.1007/s00382-018-4483-x>, 2019c.
- 1367 Meier, H. E. M., Eilola, K., Almroth-Rosell, E., Schimanke, S., Kniebusch, M., Höglund, A., Pemberton, P., Liu,
1368 Y., Väli, G., and Saraiva, S.: Disentangling the impact of nutrient load and climate changes on Baltic Sea
1369 hypoxia and eutrophication since 1850, *Clim. Dyn.*, 53, 1145–1166, <https://doi.org/10.1007/s00382-018-4296-y>,
1370 2019d.
- 1371 Meier, H. E. M., and Saraiva, S.: Projected Oceanographical Changes in the Baltic Sea until 2100, *Oxford*
1372 *Research Encyclopedia of Climate Science*, <https://doi.org/10.1093/acrefore/9780190228620.013.699>, 2020.
- 1373 Meier, H. E. M., Dieterich, C., and Gröger, M.: Natural variability is a large source of uncertainty in future
1374 projections of hypoxia in the Baltic Sea, *Commun. Earth Environ.*, 2, 50, <https://doi.org/10.1038/s43247-021-00115-9>, 2021.
- 1376 Meier, M., Andersson, H., Dieterich, C., Eilola, K., Gustafsson, B., Höglund, A., and Schimanke, S.: Transient
1377 scenario simulations for the Baltic Sea Region during the 21st century, *SMHI, Norrköping, Sweden*, 81pp,
1378 2011d.



- 1379 Mohrholz, V.: Major Baltic Inflow Statistics – Revised, *Front. Mar. Sci.*, 5,
1380 <https://doi.org/10.3389/fmars.2018.00384>, 2018.
- 1381 Neumann, T.: Climate-change effects on the Baltic Sea ecosystem: A model study, *J. Mar. Syst.*, 81, 213-224,
1382 <https://doi.org/10.1016/j.jmarsys.2009.12.001>, 2010.
- 1383 Neumann, T., Eilola, K., Gustafsson, B., Müller-Karulis, B., Kuznetsov, I., Meier, H. E. M., and Savchuk, O. P.:
1384 Extremes of temperature, oxygen and blooms in the Baltic Sea in a changing climate, *Ambio*, 41, 574-585,
1385 <https://doi.org/10.1007/s13280-012-0321-2>, 2012.
- 1386 Niiranen, S., Yletyinen, J., Tomczak, M. T., Blenckner, T., Hjerne, O., MacKenzie, B. R., Müller-Karulis, B.,
1387 Neumann, T., and Meier, H. E. M.: Combined effects of global climate change and regional ecosystem drivers
1388 on an exploited marine food web, *Global Change Biol.*, 19, 3327-3342, <https://doi.org/10.1111/gcb.12309>, 2013.
- 1389 Omstedt, A., Gustafsson, B., Rodhe, J., and Walin, G.: Use of Baltic Sea modelling to investigate the water cycle
1390 and the heat balance in GCM and regional climate models, *Clim. Res.*, 15, 95-108,
1391 <https://doi.org/10.3354/cr015095>, 2000.
- 1392 Omstedt, A., and Chen, D.: Influence of atmospheric circulation on the maximum ice extent in the Baltic Sea, *J.*
1393 *Geophys. Res-Oceans*, 106, 4493-4500, <https://doi.org/10.1029/1999JC000173>, 2001.
- 1394 Omstedt, A., Edman, M., Claremar, B., Frodin, P., Gustafsson, E., Humborg, C., Hägg, H., Mörth, M.,
1395 Rutgersson, A., Schurgers, G., and others: Future changes in the Baltic Sea acid-base (pH) and oxygen balances,
1396 *Tellus B: Chemical and Physical Meteorology*, 64, 19586, <https://doi.org/10.3402/tellusb.v64i0.19586>, 2012.
- 1397 Omstedt, A., Humborg, C., Pempkowiak, J., Perttilä, M., Rutgersson, A., Schneider, B., and Smith, B.:
1398 Biogeochemical control of the coupled CO₂-O₂ system of the Baltic Sea: a review of the results of Baltic-C,
1399 *Ambio*, 43, 49-59, <https://doi.org/10.1007/s13280-013-0485-4>, 2014.
- 1400 Oppenheimer, M., Glavovic, B. C., Hinkel, J., Wal, R. v. d., Magnan, A. K., Abd-Elgawad, A., Cai, R.,
1401 Cifuentes-Jara, M., DeConto, R. M., Ghosh, T., Hay, J., Isla, F., Marzeion, B., Meyssignac, B., and Sebesvari,
1402 Z.: Sea Level Rise and Implications for Low-Lying Islands, Coasts and Communities, in: IPCC Special Report
1403 on the Ocean and Cryosphere in a Changing Climate, edited by: Pörtner, H.-O., Roberts, D. C., Masson-
1404 Delmotte, V., Zhai, P., Tignor, M., Poloczanska, E., Mintenbeck, K., Alegria, A., Nicolai, M., Okem, A.,
1405 Petzold, J., Rama, B., and Weyer, N. M., 2019.
- 1406 Pellikka, H., Särkkä, J., Johansson, M., and Pettersson, H.: Probability distributions for mean sea level and storm
1407 contribution up to 2100 AD at Forsmark, Swedish Nuclear Fuel and Waste Management Company (SKB), 49pp,
1408 2020.
- 1409 Pihlainen, S., Zandersen, M., Hyytiäinen, K., Andersen, H. E., Bartosova, A., Gustafsson, B., Jabloun, M.,
1410 McCrackin, M., Meier, H. E. M., Olesen, J. E., Saraiva, S., Swaney, D., and Thodsen, H.: Impacts of changing
1411 society and climate on nutrient loading to the Baltic Sea, *Sci. Total Environ.*, 138935,
1412 <https://doi.org/10.1016/j.scitotenv.2020.138935>, 2020.
- 1413 Placke, M., Meier, H. E. M., Gräwe, U., Neumann, T., Frauen, C., and Liu, Y.: Long-Term Mean Circulation of
1414 the Baltic Sea as Represented by Various Ocean Circulation Models, *Front. Mar. Sci.*, 5,
1415 <https://doi.org/10.3389/fmars.2018.00287>, 2018.
- 1416 Placke, M., Meier, H. E. M., and Neumann, T.: Sensitivity of the Baltic Sea Overturning Circulation to Long-
1417 Term Atmospheric and Hydrological Changes, *J. Geophys. Res-Oceans*, 126, e2020JC016079,
1418 <https://doi.org/10.1029/2020JC016079>, 2021.
- 1419 Pushpadas, D., Schrum, C., and Daewel, U.: Projected climate change impacts on North Sea and Baltic Sea:
1420 CMIP3 and CMIP5 model based scenarios., *Biogeosci. Discuss.*, 12, [https://doi.org/10.5194/bgd-12-12229-](https://doi.org/10.5194/bgd-12-12229-2015)
1421 2015, 2015.
- 1422 Quante, M., and Colijn, F.: North Sea region climate change assessment, *Regional Climate Studies*,
1423 SpringerOpen, Cham, 2016.



- 1424 Räisänen, J., Hansson, U., Ullerstig, A., Döscher, R., Graham, L. P., Jones, C., Meier, H. E. M., Samuelsson, P.,
1425 and Willén, U.: European climate in the late twenty-first century: regional simulations with two driving global
1426 models and two forcing scenarios, *Clim. Dyn.*, 22, 13-31, <https://doi.org/10.1007/s00382-003-0365-x>, 2004.
- 1427 Reckermann, M., Omstedt, A., Soomere, T., Aigars, J., Akhtar, N., Bełdowski, J., Brauwer, C. P.-S. d., Cronin,
1428 T., Czub, M., Eero, M., Hyttiäinen, K., Jalkanen, J.-P., Kiessling, A., Kjellström, E., Larsén, X. G., McCrackin,
1429 M., Meier, H. E. M., Oberbeckmann, S., Parnell, K., Poska, A., Saarinen, J., Szymczycha, B., Undeman, E.,
1430 Viitasalo, M., Wörman, A., and Zorita, E.: Human impacts and their interactions in the Baltic Sea region, *Earth
1431 Syst. Dynam. Discuss.*, 1-127, <https://doi.org/10.5194/esd-2021-54>, 2021.
- 1432 Rummukainen, M., Räisänen, J., Bringfelt, B., Ullerstig, A., Omstedt, A., Willén, U., Hansson, U., and Jones,
1433 C.: A regional climate model for northern Europe: model description and results from the downscaling of two
1434 GCM control simulations, *Clim. Dyn.*, 17, 339-359, <https://doi.org/10.1007/s003820000109>, 2001.
- 1435 Rummukainen, M., Bergström, S., Persson, G., Rodhe, J., and Tjernström, M.: The Swedish Regional Climate
1436 Modelling Programme, SWECLIM: A Review, *Ambio* 33, 176-182, 177, 2004.
- 1437 Rutgersson, A., Jaagus, J., Schenk, F., Stendel, M., Barring, L., Briede, A., ClaremarInger, B., Hanssen-Bauer,
1438 Holopainen, J., Moberg, A., Nordli, Ø., Rimkus, E., and Wibig, J.: Recent Change - Atmosphere, in: *Second
1439 Assessment of Climate Change for the Baltic Sea Basin*, edited by: BACC II Author Team, *Regional Climate
1440 Studies*, Springer International Publishing, Cham, 69-97, https://doi.org/10.1007/978-3-319-16006-1_4, 2015.
- 1441 Ryabchenko, V. A., Karlin, L. N., Isaev, A. V., Vankevich, R. E., Eremina, T. R., Molchanov, M. S., and
1442 Savchuk, O. P.: Model estimates of the eutrophication of the Baltic Sea in the contemporary and future climate,
1443 *Oceanology+*, 56, 36-45, <https://doi.org/10.1134/S0001437016010161>, 2016.
- 1444 Samuelsson, P., Jones, C. G., Willén, U., Ullerstig, A., Gollvik, S., Hansson, U. L. F., Jansson, C., Kjellström,
1445 E., Nikulin, G., and Wyser, K.: The Rossby Centre Regional Climate model RCA3: model description and
1446 performance, *Tellus A: Dynamic Meteorology and Oceanography*, 63, 4-23, [https://doi.org/10.1111/j.1600-
0870.2010.00478.x](https://doi.org/10.1111/j.1600-
1447 0870.2010.00478.x), 2011.
- 1448 Saraiva, S., Meier, H. E. M., Andersson, H., Höglund, A., Dieterich, C., Gröger, M., Hordoir, R., and Eilola, K.:
1449 Uncertainties in Projections of the Baltic Sea Ecosystem Driven by an Ensemble of Global Climate Models,
1450 *Front. Earth Sci.*, 6, <https://doi.org/10.3389/feart.2018.00244>, 2019a.
- 1451 Saraiva, S., Meier, H. E. M., Andersson, H., Höglund, A., Dieterich, C., Gröger, M., Hordoir, R., and Eilola, K.:
1452 Baltic Sea ecosystem response to various nutrient load scenarios in present and future climates, *Clim. Dyn.*, 52,
1453 3369-3387, <https://doi.org/10.1007/s00382-018-4330-0>, 2019b.
- 1454 Savchuk, O. P., Larsson, U., and Elmgren, L.: Secchi depth and nutrient concentration in the Baltic Sea: model
1455 regressions for MARE's Nest, Department of Systems Ecology, Stockholm University, Sweden, Technical
1456 Report, 12pp, 2006.
- 1457 Schimanke, S., Meier, H. E. M., Kjellström, E., Strandberg, G., and Hordoir, R.: The climate in the Baltic Sea
1458 region during the last millennium simulated with a regional climate model, *Clim. Past*, 8, 1419,
1459 <https://doi.org/10.5194/cp-8-1419-2012>, 2012.
- 1460 Schimanke, S., and Meier, H. E. M.: Decadal-to-Centennial Variability of Salinity in the Baltic Sea, *J. Climate*,
1461 29, 7173-7188, <https://doi.org/10.1175/JCLI-D-15-0443.1>, 2016.
- 1462 Sen, P. K.: Estimates of the Regression Coefficient Based on Kendall's Tau, *J. Am. Stat. Assoc.*, 63, 1379-1389,
1463 <https://doi.org/10.1080/01621459.1968.10480934>, 1968.
- 1464 Sjöberg, B.: Sea and coast. National atlas of Sweden, 1992.
- 1465 Skogen, M. D., Eilola, K., Hansen, J. L. S., Meier, H. E. M., Molchanov, M. S., and Ryabchenko, V. A.:
1466 Eutrophication status of the North Sea, Skagerrak, Kattegat and the Baltic Sea in present and future climates: A
1467 model study, *J. Mar. Syst.*, 132, 174-184, <https://doi.org/10.1016/j.jmarsys.2014.02.004>, 2014.



- 1468 Suursaar, Ü., and Sooäär, J.: Decadal variations in mean and extreme sea level values along the Estonian coast of
1469 the Baltic Sea, *Tellus A: Dynamic Meteorology and Oceanography*, 59, 249-260, <https://doi.org/10.1111/j.1600-0870.2006.00220.x>, 2007.
- 1471 Suursaar, Ü.: Combined impact of summer heat waves and coastal upwelling in the Baltic Sea, *Oceanologia*, 62,
1472 511-524, <https://doi.org/10.1016/j.oceano.2020.08.003>, 2020.
- 1473 Taylor, K. E., Stouffer, R. J., and Meehl, G. A.: An Overview of CMIP5 and the Experiment Design, *Bull.*
1474 *Amer. Meteor. Soc.*, 93, 485-498, <https://doi.org/10.1175/BAMS-D-11-00094.1>, 2012.
- 1475 Theil, H.: A rank-invariant method of linear and polynomial regression analysis, 3, *Indagat. Math.*, 1, 1397-
1476 1412, 1950.
- 1477 Uppala, S. M., KÅllberg, P. W., Simmons, A. J., Andrae, U., Bechtold, V. D. C., Fiorino, M., Gibson, J. K.,
1478 Haseler, J., Hernandez, A., Kelly, G. A., Li, X., Onogi, K., Saarinen, S., Sokka, N., Allan, R. P., Andersson, E.,
1479 Arpe, K., Balmaseda, M. A., Beljaars, A. C. M., Berg, L. V. D., Bidlot, J., Bormann, N., Caires, S., Chevallier,
1480 F., Dethof, A., Dragosavac, M., Fisher, M., Fuentes, M., Hagemann, S., Hólm, E., Hoskins, B. J., Isaksen, L.,
1481 Janssen, P. A. E. M., Jenne, R., McNally, A. P., Mahfouf, J.-F., Morcrette, J.-J., Rayner, N. A., Saunders, R. W.,
1482 Simon, P., Sterl, A., Trenberth, K. E., Untch, A., Vasiljevic, D., Viterbo, P., and Woollen, J.: The ERA-40 re-
1483 analysis, *Q. J. Roy. Meteor. Soc.*, 131, 2961-3012, <https://doi.org/10.1256/qj.04.176>, 2005.
- 1484 Vihma, T., and Haapala, J.: Geophysics of sea ice in the Baltic Sea: A review, *Prog. Oceanogr.*, 80, 129-148,
1485 <https://doi.org/10.1016/j.pcean.2009.02.002>, 2009.
- 1486 Vuorinen, I., Hänninen, J., Rajasilta, M., Laine, P., Eklund, J., Montesino-Pouzols, F., Corona, F., Junker, K.,
1487 Meier, H. E. M., and Dippner, J. W.: Scenario simulations of future salinity and ecological consequences in the
1488 Baltic Sea and adjacent North Sea areas—implications for environmental monitoring, *Ecol. Indic.*, 50, 196-205,
1489 <https://doi.org/10.1016/j.ecolind.2014.10.019>, 2015.
- 1490 Wang, J., Yang, B., Ljungqvist, F. C., Luterbacher, J., Osborn, Timothy J., Briffa, K. R., and Zorita, E.: Internal
1491 and external forcing of multidecadal Atlantic climate variability over the past 1,200 years, *Nat. Geosci.*, 10, 512-
1492 517, <https://doi.org/10.1038/ngeo2962>, 2017.
- 1493 Wang, S., Dieterich, C., Döscher, R., Höglund, A., Hordoir, R., Meier, H. E. M., Samuelsson, P., and
1494 Schimanke, S.: Development and evaluation of a new regional coupled atmosphere–ocean model in the North
1495 Sea and Baltic Sea, *Tellus A: Dynamic Meteorology and Oceanography*, 67, 24284,
1496 <https://doi.org/10.3402/tellusa.v67.24284>, 2015.
- 1497 Weigel, B., Andersson, H. C., Meier, H. E. M., Blenckner, T., Snickars, M., and Bonsdorff, E.: Long-term
1498 progression and drivers of coastal zoobenthos in a changing system, *Mar. Ecol. Prog. Ser.*, 528, 141-159,
1499 <https://doi.org/10.3354/meps11279>, 2015.
- 1500 Weisse, R., and Hünicke, B.: Baltic Sea Level: Past, Present, and Future, *Oxford Research Encyclopedia of*
1501 *Climate Science*, Oxford University Press, 2019.
- 1502 Zandersen, M., Hyytiäinen, K., Meier, H. E. M., Tomczak, M. T., Bauer, B., Haapasaari, P. E., Olesen, J. E.,
1503 Gustafsson, B. G., Refsgaard, J. C., Fridell, E., Pihlainen, S., Le Tissier, M. D. A., Kosenius, A.-K., and Van
1504 Vuuren, D. P.: Shared socio-economic pathways extended for the Baltic Sea: exploring long-term environmental
1505 problems, *Reg. Environ. Change*, 19, 1073-1086, <https://doi.org/10.1007/s10113-018-1453-0>, 2019.
- 1506 Zillén, L., and Conley, D. J.: Hypoxia and cyanobacteria blooms—are they really natural features of the late
1507 Holocene history of the Baltic Sea?, *Biogeosciences*, 7, 2567, <https://doi.org/10.5194/bg-7-2567-2010>, 2010.